

**Technical Report
TR-1109**

Channel Characterization for EHF Satellite Communications on the Move

W.M. Smith

12 July 2006

Lincoln Laboratory
MASSACHUSETTS INSTITUTE OF TECHNOLOGY
LEXINGTON, MASSACHUSETTS



Prepared for the Department of the Army under Air Force Contract FA8721-05-C-0002.

Approved for public release; distribution is unlimited.

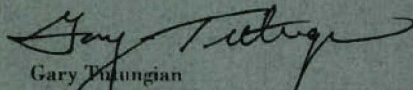
This report is based on studies performed at Lincoln Laboratory, a center for research operated by Massachusetts Institute of Technology. This work was sponsored by the Department of the Army, SFAE-C3T-WINT-TMD, under Air Force Contract FA8721-05-C-0002.

This report may be reproduced to satisfy needs of U.S. Government agencies.

The ESC Public Affairs Office has reviewed this report, and it is releasable to the National Technical Information Service, where it will be available to the general public, including foreign nationals.

This technical report has been reviewed and is approved for publication.

FOR THE COMMANDER


Gary Thungian
Administrative Contracting Officer
Plans and Programs Directorate
Contracted Support Management

Non-Lincoln Recipients

PLEASE DO NOT RETURN

Permission has been granted to destroy this document, when it is no longer needed.

Massachusetts Institute of Technology
Lincoln Laboratory

Channel Characterization for
EHF Satellite Communications on the Move

W.M. Smith
Group 63

Technical Report 1109

12 July 2006

Approved for public release; distribution is unlimited.

Lexington

Massachusetts

ABSTRACT

In addition to long signal propagation delays, the mobile satellite terminal in a land-mobile satellite communications system is subject to channel impairments imposed by the terrestrial environment. Statistical channel models are needed for protocol development and performance evaluation of systems for satellite communications (SATCOM) on the move.

Experimental measurements were made in and around Boston, MA, using a prototype system for SATCOM on the move. The measurements characterize the 20 GHz down-link signal and were made in the fall and winter months of 2004. The elevation angle to the satellite was approximately 36° . This report covers the measurement campaign, initial single-terminal channel modeling, and multi-terminal channel models relevant for cooperating ground terminals.

The data sets are analyzed for the statistical properties of the channel state. The channel is considered to be “open” when a clear path exists to the satellite and “blocked” when there is an obstruction in the path that prevents the successful transfer of information from transmitter to receiver. For the single-channel analysis, three operational environments were previously classified as urban, rural, or open. We propose two new operational categories: open highway and dense urban. The addition of these categories is based on a natural partitioning of the experimental data. The open highway channel model contains very long open intervals, 310 m on average, and is blocked 5% of the time. The dense urban environment, on the other hand, consists of tall, closely spaced buildings. In this environment, the average blockage duration is 130 m and the channel is blocked 89% of the time. We evaluate the suitability of Markov state models to accurately reflect the channel behavior.

The effectiveness of using multiple terminals to maximize the use of a single satellite depends on the correlation properties of the blockage events experienced by each mobile ground terminal. Terminal groups with uncorrelated channel outages are able to maximize the use of the satellite since there is a lower probability that all terminals are simultaneously blocked. The autocorrelation properties of the blockage channel state determine how closely spaced the ground terminals may be in order to reap the full benefits of spatial diversity. We derive the correlation coefficient of a multiple-state Markov channel with arbitrary state outputs. The correlation coefficient of the two-state model is found to be exponential, regardless of the state output values. We find the empirical channel decorrelation distance to be from 10 m to 100 m, depending on the operating environment. The empirical blockage probability reduces from 40% to 5% for a cluster of four randomly moving ground terminals in a light urban environment.

ACKNOWLEDGMENTS

Financial support for this project is gratefully acknowledged. The Program Manager, Warfighter Information Network-Tactical (PM WIN-T) supported the development of the prototype vehicle used for the measurement campaign described in this report. The analysis of the measurement data was also supported in part by a Science and Technology Objective administered by the Army's Communications and Electronics Command (CECOM).

Many people contributed in different ways to the success of this project. I am indebted to Andrew Worthen and John Choi for their careful reading of this manuscript and for numerous suggestions for improvement during the data analysis. I would also like to thank Jeff Schodorf for his useful ideas for planning the measurement campaign and for his helpful comments regarding the analysis and interpretation of some of the measurement data.

The measurement campaign would not have been possible without the superb handling of the test vehicle, both in the shop and in the field, by Ted O'Connell. I am grateful for the support of the following people in setting up the experiment and debugging technical issues with the setup: Marie Heath, Tim Schiefelbein, John Murphy, John Delisle, Curran Nachbar, Jason Hillger, and Marc Siegel.

TABLE OF CONTENTS

Abstract	iii
Acknowledgments	v
List of Illustrations	ix
List of Tables	xi
1. INTRODUCTION	1
1.1 Motivation	1
1.2 Report Outline	4
2. EXPERIMENT	5
2.1 Experiment Objectives	5
2.2 Experiment Configuration	6
2.3 Test Locations	8
2.4 Metrics and Data Reduction	9
3. BLOCKAGE MODELING	13
3.1 Channel Models	13
3.2 Qualitative Observations	14
3.3 Analysis	18
3.4 Guidelines for Partitioning Data Sets	18
3.5 Parameters for Markov Models	21
3.6 Summary	28
4. MULTIPLE-TERMINAL TECHNIQUES	29
4.1 Blockage Properties for Multiple Cooperating Ground Terminals	29
4.2 Autocorrelation Properties of a Two-state Markov Process	35
4.3 Empirical Results for Autocorrelation of SATCOM On-the-Move Blockage Channels	37
4.4 Summary	39
5. CONCLUSION	41
5.1 Report Summary	41
5.2 Future Work	41
References	43

LIST OF ILLUSTRATIONS

Figure No.		Page
1	Lincoln Laboratory SATCOM on-the-move prototype	1
2	Channel blockage	2
3	Prototype node architecture	3
4	Experiment setup	6
5	Protocol stack view	7
6	Measurement locations	10
7	Data capture points	11
8	Signal strength estimator block diagram	11
9	Time-series examples	12
10	Signal strength measurements in Cambridge, MA	15
11	Signal strength measurements in Boston, MA	16
12	Signal strength measurements in Devens, MA	17
13	Summary distributions of blocked and open intervals	19
14	Distributions of blocked and open intervals for Cambridge data sets	20
15	Distributions of blocked and open intervals for Boston data sets	21
16	The two-state Markov model	21
17	Parameter matching for Markov channel state models	25
18	Independent routes used for spatial and time domain analyses	30
19	Blockage and connection probabilities of scattered cooperating terminals using spatial and time domain analyses	31
20	Blockage and connection duration probabilities of cooperating terminals in convoy with (a) constant speed and fixed-distance separation between vehicles and (b) variable speed and fixed time separation between vehicles	33
21	Average blocked and open durations for scattered cooperating nodes	34
22	Average blocked and open durations for cooperating nodes in convoy	34
23	Summary of two-state Markov model with correlation coefficients	38
24	Measured decorrelation distances	40

LIST OF TABLES

Table No.		Page
1	Mobile Terminal Parameters	7
2	Test Locations	8
3	Summary of Blockage Statistics	20
4	Parameters Using the Two-State Markov Model	23
5	Parameters Using the Gilbert Model with Connection Duration Only	23
6	Parameters Using the Gilbert Model, Jointly Fitting Blockage and Connection Durations	24

1. INTRODUCTION

1.1 MOTIVATION

Satellite communications (SATCOM) on the move (OTM) is becoming an increasingly important application for the U.S. military. With more rapid deployments and a highly mobile force, communication is needed within battle theaters, where no terrestrial communication infrastructure may be used. Furthermore, the battlefield objective may be so short in duration that setting up a terrestrial communications infrastructure is not feasible.



Figure 1. Lincoln Laboratory SATCOM on-the-move prototype. Challenges encountered by satellite communication on the move include antenna pointing, time tracking, ruggedized components, and link throughput degraded by blocked channels.

The components used in land-mobile, satellite ground terminals, such as the one pictured in Figure 1, must be ruggedized to withstand the vibrations caused by vehicle motion. In addition to the usual RF and antenna components, the SATCOM OTM terminal must contain additional components that will assist in maintaining the communication link to the satellite while the vehicular ground terminal is mobile. A navigation unit is required to provide vehicle location information so that the terminal can point the antenna in the proper direction. The pointing subsystem must be rugged enough to compensate for vehicle motion. Finally, tracking systems—both spatial and temporal—must be implemented to maintain the connection with the satellite. The spatial tracking requirement is obvious, but the time tracking requirements are increasingly important for wideband, protected SATCOM with higher signaling rates.

The mobility of the ground terminal introduces technical challenges for the end-to-end system design. Because of the high gain required to communicate with a satellite, the radiation pattern of the satellite antenna is highly directional. Since the antenna pattern is highly directional, the communication channel is usually considered to be in one of two states: open or blocked. In the “open” state, the path to the satellite is free of obstructions and data is successfully transmitted over the link. In the “blocked” state, the path to the satellite is obstructed by building, trees, or other objects in the environment, preventing the successful transmission of data.

In addition to the deep fades in signal strength with potentially long durations, the mobile terminal in a land-mobile, satellite communications system is subject to long signal propagation delays resulting from the round-trip transit time to the satellite on orbit. The statistical properties of the outages experienced by the mobile ground terminal determine which mitigation techniques will be effective. These techniques, coupled with the long delays, determine how well the end-to-end communications system will perform.

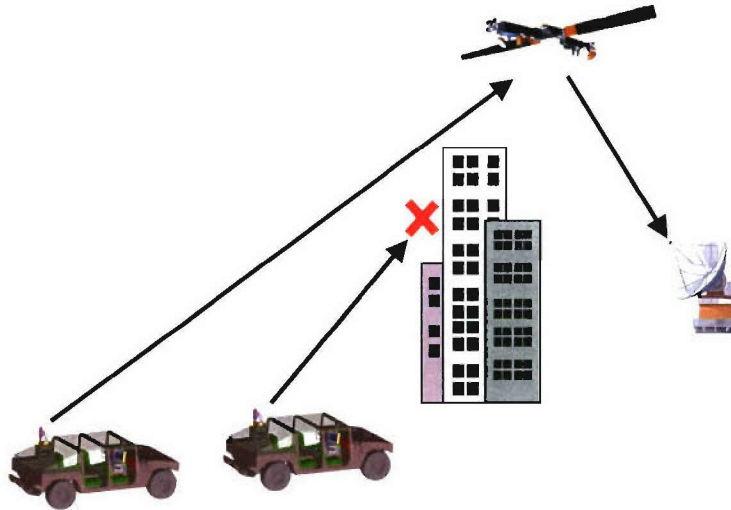


Figure 2. Channel blockage. By channel blockage, we refer to the condition in which the primary propagation path to the satellite is blocked by an obstruction in the environment.

Blockage of the propagation path to the satellite, as illustrated in Figure 2, results in outages at the physical layer, during which time no data may be decoded. To fully utilize the channel, upper-layer protocols must react to these outages. The duration of outage events and the frequency at which they occur impact the design of protocols and how well they perform in these environments.

Statistical models are needed for protocol development and for off-line emulation and analysis of system performance. The model should be derived from data collected using an actual working SATCOM OTM system. The parameters for the model should span the range of environments of probable operating

conditions. The channel model must match the characteristics of the environment for which it is used. The long, deep fades encountered during outage events leads to the use of blocked channel models. Finally, a successful model will be generative, *i.e.*, the statistics of the synthesized data should match those of the measured data.

The Lincoln Laboratory approach to SATCOM on the move has been to build a prototype system, perform experiments, and incorporate lessons learned from the entire process into a subsequent, more capable prototype. In 2002, a SATCOM OTM system was developed at Lincoln Laboratory. This system was the first EHF SATCOM OTM system demonstrated. A report summarizing the results of a measurement campaign conducted at the end of the prototype development cycle was written by Schodorf [1]. The operating locations for those experiments were organized into three broad categories: urban, rural, and open environments. The terminal used for the experiments described by [1] had some limitations with respect to the duration of outages it could withstand while still maintaining connection to the satellite.

In the subsequent two years, the lessons learned from those initial experiments were incorporated into a second SATCOM OTM terminal. In addition to having a higher downlink data rate capability, the second terminal has an improved design for modularity. The aperture and RF subsystem are modular, as shown in the architecture diagram in Figure 3, and can support multiple frequency bands, although not simultaneously. A rubidium oscillator is used as a more precise time reference, and, along with an improved time-tracking algorithm, the terminal can recover from much longer outages without dropping the communications link than can the previous prototype. As a result, experiments that are longer in duration may be conducted in new environments containing more channel obstructions. This report documents the results of the measurements collected with this second SATCOM OTM terminal.

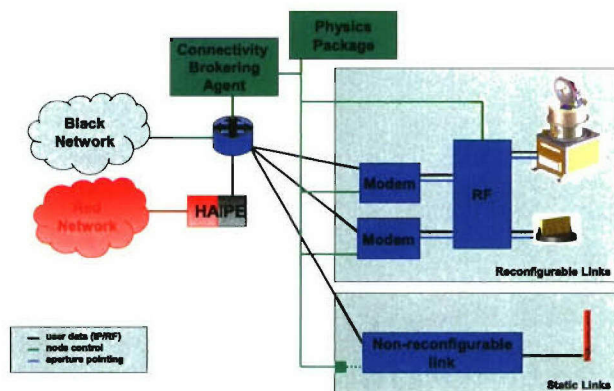


Figure 3. Prototype node architecture. The modular architecture provides a mix-and-match selection of modems and antennas.

1.2 REPORT OUTLINE

The remainder of this report is organized as follows:

Chapter 2 outlines the experiment objectives. These experiments build on the experience gained by Schodorf [1]. We describe the vehicle configuration, noting the improvements made over the previous prototype. The experiment locations were chosen to be representative of a wide range of probable operating conditions for SATCOM on the move. We identify the experiment locations and describe the characteristics of environments that were not previously studied.

Chapter 3 presents Markov models that may be used to describe the blockage channel for SATCOM on the move. The Markov models provide a simple, compact way of representing the blockage channel. We review previous blockage models applied to the new data and discuss the advantages and limitations of using these models for emulation and simulation.

Multiterminal techniques are discussed in Chapter 4. Having multiple ground nodes cooperatively communicate with the same satellite can overcome some of the channel impairments and improve overall system performance. The channel measurements are used to evaluate the theoretical performance of cooperative strategies.

Finally, conclusions are drawn in Chapter 5.

2. EXPERIMENT

2.1 EXPERIMENT OBJECTIVES

The objective of the experiments conducted with the SATCOM on-the-move terminal prototype is to capture the channel characteristics over a wide range of operating conditions. The measurements captured in this campaign are an extension of previous work by Schodorf [1]. Due to the improved stability of the SATCOM terminal prototype used for these experiments, the data sets are typically longer in duration, cover larger geographical areas, and include regions with higher blockage fractions than those reported by [1]. The objectives of this measurement campaign described in this report are as follows:

1. Expand Library of SATCOM On-the-Move Channel Measurements.

The data set from this measurement campaign expands the library of physical channel measurements upon which current statistical models are based for SATCOM on the move. Using lessons learned from previous terminal designs, the terminal used for these experiments has improved time-tracking capabilities so that it can maintain better time synchronization with the satellite. This improved time synchronization enables longer experiments to be conducted in harsher environments since the terminal can withstand longer channel outages without breaking its session with the satellite.

2. Refine Statistical Channel Models

The expanded data sets gathered from larger geographical areas are needed to refine the parameters of existing statistical models. Longer experiments are used to provide larger data sets upon which to base statistical models of the physical channel. Furthermore, since measurements in this data set cover new environments, models can be defined to cover a broader range of operating conditions.

3. Performance of TCP over SATCOM On the Move

For each experiment, a TCP data stream flows from a server at the stationary terminal to the vehicle node. The behavior of this data flow can be evaluated in each operating environment.

4. Link-level Error Models

By logging raw data bits that are sent and received from each end of the satellite link, an offline comparison can be used to reconstruct errors due to channel impairments. The error patterns from this offline analysis can be used to replay these experiment scenarios under tight control in network emulations.

5. Study the Effects of Seasonal Variation

One long-term goal of this study is to model the seasonal effects of foliage on the SATCOM on-the-move channel. This data set includes measurements taken in the fall and winter months and should be directly compared to measurements taken in the spring and summer months.

Although this report focuses primarily on objectives 1 and 2 listed above, the measurement data set includes some data from objective 4. The remaining items are to be studied separately and potentially included in other reports.

2.2 EXPERIMENT CONFIGURATION

The experiment setup for the channel measurements described in this report is shown in Figure 4. The configuration consists of a control center with a server that provides data flows to a HMMWV over a satellite communication channel. The forward link supports a medium data rate (MDR) 256 kbps downlink to the vehicle. The return link to the control center supports low data rate (LDR) channels running at either 2.4 or 4.8 kbps. The 20 GHz downlink channel is measured for the channel characterizations presented in this report. The output of an energy estimator in the demodulator is used as a signal strength metric.

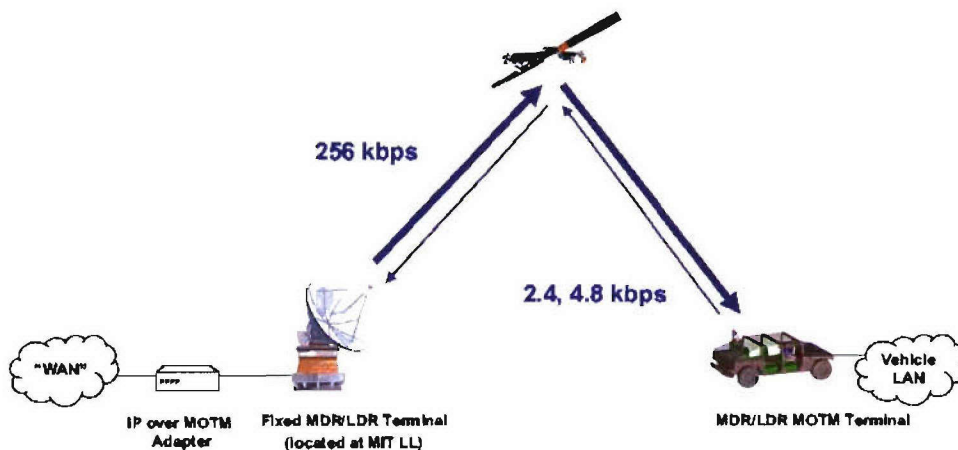


Figure 4. Experiment setup. Experiments include a stationary terminal and a mobile vehicle terminal. The forward link supports 256 kbps to the vehicle and either 2.4 kbps or 4.8 kbps back to the stationary terminal.

The vehicle contains a mobile satellite terminal with a tracking antenna and a client computer to initiate the data flows and to log the system performance. The look angle to the satellite is approximately 36° . The antenna positioner tracks the satellite using an active control system with the aid of an inertial navigation unit. Most of the measurements were made on improved roads where the antenna positioner is known to have adequate performance so as not to degrade the communication quality of the link. In off-road locations, however, pointing errors contribute to link outages, and those outages are included in the results here.

The operating conditions of the mobile terminal node are outlined in Table 1. Each experiment begins by establishing the link to the satellite by both terminals. This is usually done while the vehicle is stationary, but acquisition can be done on the move so long as the path to the satellite remains unblocked.

TABLE 1
Mobile Terminal Parameters

Downlink Frequency	20.2 – 21.2 GHz
Satellite Elevation Angle	$\approx 36^\circ$
Downlink Data Rate	256 kbps
Uplink Data Rate	2.4 kbps or 4.8 kbps
End-to-End RF Gain	≈ 100 dB

An IP protocol stack is configured at each end of the link as shown in Figure 5. The green layers in Figure 5 are Lincoln Laboratory-specific Linux kernel modules that constitute the experimental protocol stack (XPS). These modules are responsible for serializing the IP protocol for transport over satellite. Also included in the XPS implementation is a windowed, selective repeat automatic repeat request (ARQ) protocol. More information on XPS and the performance of the link-layer protocol can be found in [2, 3].

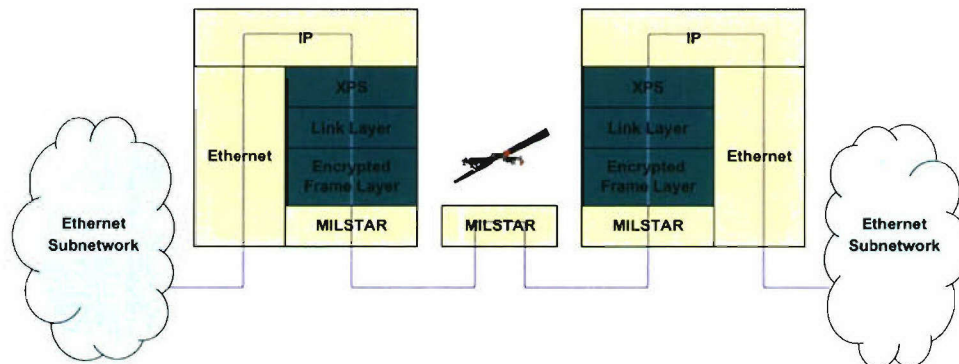


Figure 5. Protocol stack view. Linux routers run at each end of the link to serialize the IP traffic to pass over the MILSTAR link.

Accurate signal timing must be maintained during channel outages so that the terminal can once again decode the received signal rather than drop the connection when the signal returns. The measurement terminal used in this experiment uses the rubidium oscillator as a time reference and uses the output of the inertial navigation system to compensate for vehicle movement during long outages. Using these compensation techniques, the terminal can maintain signal timing precise enough to recover from long outage periods. This robustness permits data collection in areas that were previously unmeasurable with a less capable terminal.

2.3 TEST LOCATIONS

Measurements were made from the end of October to the middle of December 2004. During this time period, most of the leaves had already fallen off the trees. The measurement locations include the urban areas of Hartford, CT, Boston, MA, and Cambridge, MA. Each urban area is unique in its makeup. Boston consists of tall, closely spaced, high-rise office buildings in the financial district. Surrounding the financial district are areas of smaller buildings and more trees. Cambridge has a smaller downtown section with a lower density of tall buildings. Surrounding downtown Cambridge are residential areas with trees and small buildings. Hartford also has a small downtown area with high-rise office buildings.

Rural, tree-lined highways in the western suburbs of Boston and the paved and off-road courses at Ft. Devens exhibit the effects of foliage and tree cover. A route through Concord, MA, and surrounding towns consists of a two-lane road with dense tree cover for most of the route. The data from Ft. Devens include measurements that were taken on improved and unimproved roads and through a variety of densities of tree cover. The open highway data set includes measurements taken on multilane interstate highways between Boston, MA, and Hartford, CT. The operating areas are shown in Figure 6 and summarized in Table 2.

TABLE 2
Test Locations

Location	Description of Environment
Boston, MA	tall, closely spaced buildings little or no foliage in financial district
Cambridge, MA	shorter, less densely spaced buildings some residential areas with foliage and buildings 2–3 stories
Concord, MA	rural/suburban area two-lane roads lined with trees
Devens, MA	rural; improved and unimproved roads
Open Highway	divided, limited-access highways

These locations are slightly different from the open, rural, and urban environments used by [1]. The Cambridge, MA, measurements are the most similar to the urban environment of [1]. The Boston, MA,

measurements and the open highway environment represent extremes not captured by the open, rural, and urban classifications. The open highway data set consists primarily of regions in which the connection to the satellite is much longer in duration than in any of the other environments. The Boston data set includes regions with much higher blockage fractions than any of the previously reported environments. For preciseness, in this report we will refer to each data set by its particular location.

2.4 METRICS AND DATA REDUCTION

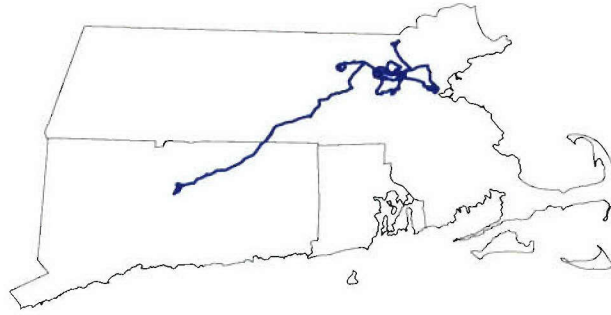
The metrics captured during each experiment are illustrated in Figure 7. The encrypted bits sent and received over the air are logged for link-layer analysis. The data for this report, however, are collected from an energy estimator in the demodulator. The energy estimate is obtained in the demodulation stage of the mobile terminal modem. The energy estimator is shown in Figure 8. The energy metric is derived from the correlator outputs in the time-tracking loop. The correlators are used to adjust the signal timing to match that of the downlink synchronization hop bits. The correlator output values are calibrated and give an estimate of the received signal-to-noise ratio at the demodulator. A more complete description of the correlator operation is given by Delisle [4].

The data is recorded as follows to facilitate post-test analysis: The vehicle's position is recorded from the inertial navigation system. Periodic timestamps and position (latitude and longitude) values are stored in log files. In between these waypoints, the signal strength metrics from the receiver are logged. For analysis, a timestamp and its associated location values are interpolated for each signal strength estimate from the waypoint anchors. This time tagging is done for each metric recorded (signal strength, latitude, longitude, pointing angles, etc). Through the remainder of this report, the logged values for position and time are referred to as time-based samples. Some examples of these time-series signal strength plots are included in Figure 9.

Time-series analysis is specific for a certain vehicle velocity profile through a given test area. For example, traversing an intersection without stopping produces a different time-series result than when the vehicle stops at a light. Likewise, traveling at a slower speed will produce blockage phenomena that are longer in temporal duration. To remove this dependence on time-varying velocity profiles, the analysis can be done in the spatial domain.

For spatial analysis, the following steps are taken to remove the dependence on the velocity profile in the raw data:

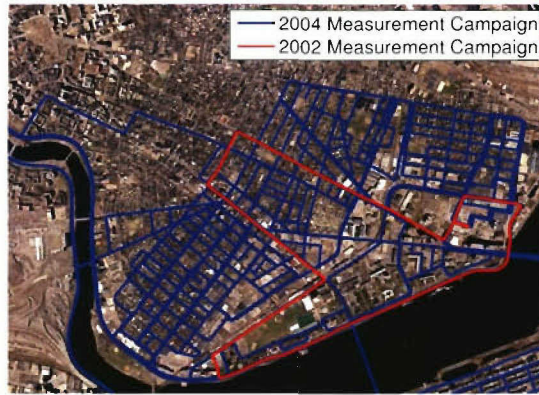
1. The latitude and longitude values are converted to linear distance units. This is achieved by projecting the interpolated location of each sample onto the Massachusetts State Plane.
2. Based on the maximum speed the vehicle achieves in a particular data set, a spatial sampling interval, D_{samp} , is chosen such that at least one time-series sample exists for each spatial sample.
3. The linear distance traveled by the vehicle is broken into segments, all of which are D_{samp} in length.
4. All time-series signal strength power samples in a single D_{samp} interval are averaged together to produce a single measurement for each spatial sampling interval.



(a) All measurement locations



(b) Devens, MA



(c) Cambridge, MA



(d) Boston, MA, downtown



(e) Boston, MA, Back Bay

Figure 6. Measurement locations. The 2004 measurement campaign covered many locations in and around Boston, MA, as well as highway environments between Lexington, MA, and Hartford, CT. The data sets for Cambridge, MA, and Devens, MA, are substantially increased from the 2002 measurement campaign. The measurements in Boston, the Back Bay, and on the open highway are new data sets.

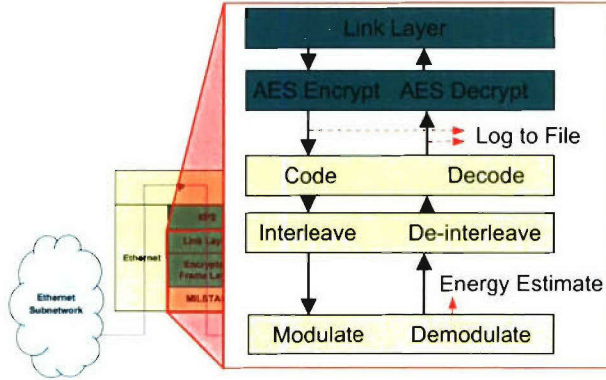


Figure 7. Data capture points. Energy estimates come from the demodulator in the vehicle modem. Link-level bits, both sent and received, are logged between the encrypt/decrypt and the code/decode stages.

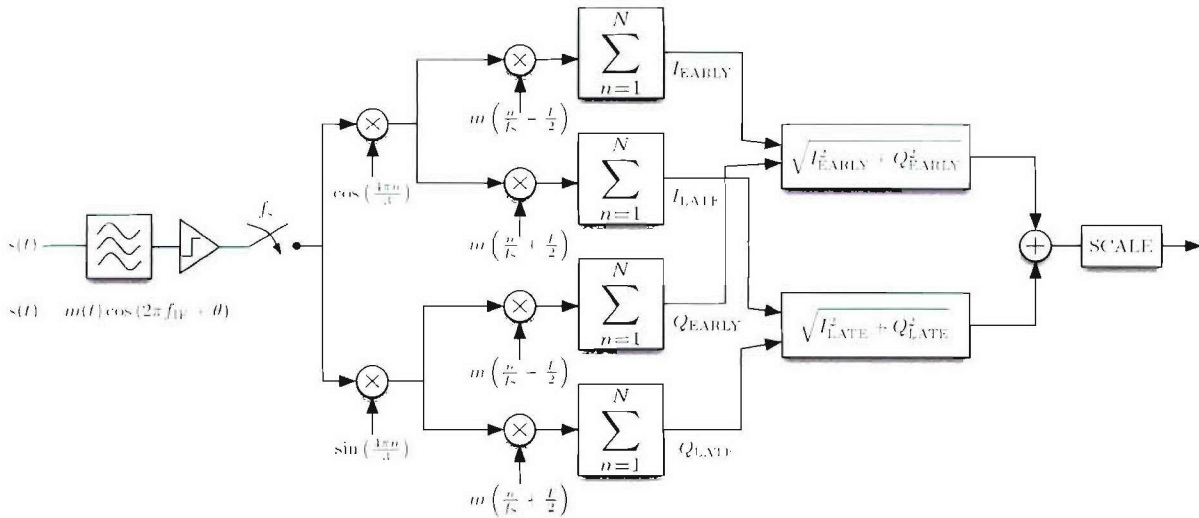
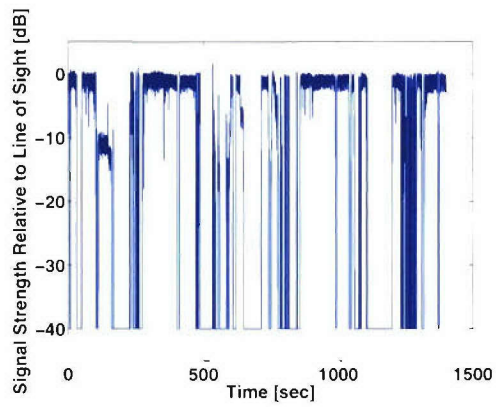
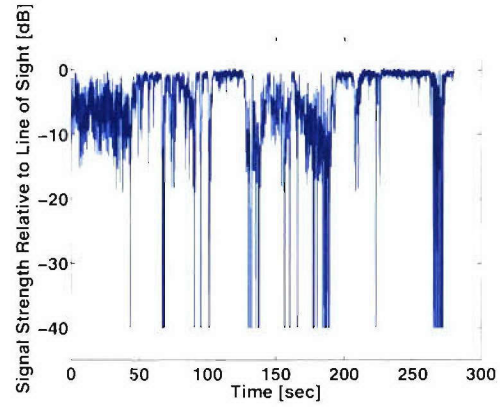


Figure 8. Signal strength estimator block diagram. The signal strength estimate is derived from the early and late correlation values computed in the time-tracking loop of the receiver.



(a) Boston, MA



(b) Devens, MA

Figure 9. Time-series examples. Shown here are two examples of signal strength measurements vs. time. The severity of the blockages by buildings is shown in (a). An example of foliage-induced blockage is shown in (b)

3. BLOCKAGE MODELING

Models of the channel blockage behavior are needed for evaluation of system performance in emulation or simulation. For the channel model to reflect the system behavior in operational environments, it must be based on physical measurements made in those environments. In this section, we present results of the measurement campaign with the Lincoln Laboratory SATCOM on-the-move prototype vehicle. We begin by making some qualitative observations of the data. These qualitative observations lead to a natural grouping of the data. We quantitatively analyze each grouping. We evaluate the ability of existing models to represent the statistical nature of the recorded data.

3.1 CHANNEL MODELS

Different approaches have been used in the past to model the SATCOM on-the-move channel. Loo and Butterworth [5] give an overview of modeling envelope and phase variations for the channel. Abdi *et al.* [6] and Dovič *et al.* [7] introduce new statistical small-scale fading models, while Döttling *et al.* [8] and Oestges and Vanhoenacker-Janvier [9] take a more deterministic approach with ray tracing.

Markov models are appealing because of their simplicity and their ability to model a fundamental change in state of the underlying system. Gilbert [10] used Markov models to describe the behavior of burst errors on a telephone line. Similarly, the loss of signal strength from the satellite in a SATCOM on-the-move system results in bursts of errors when decoding the received signal.

More recently, others [1, 11, 12, 13] have had reasonable success in modeling the SATCOM on-the-move channel as being in states with two or three degrees of freedom governed by Markov models. Schodorf [1] models the channel state using a simple two-state Markov model and an augmented Gilbert-Elliot model. Yao [13] introduces a three-state model and uses memory decay curves to capture the characteristics of channel memory. The blockage models used in this chapter and the autocorrelation analysis in Chapter 4 are extensions of the work by [1] and [13].

We examine the statistics of blockage for new data sets that have been collected in the vicinity of Boston, MA. We use a threshold of 5 dB below the line-of-sight signal strength to divide our observed signal strength into blocked and unblocked states. While 5 dB is more than the excess signal margin on the satellite-to-ground link for the particular modulation and coding mode we were using, it was sufficient to eliminate false blocked state indications due to noisy signal strength estimates when operating in unblocked conditions. Throughout the remainder of this report, we will refer to locations in which the signal is above this -5 dB threshold as being “unblocked” or in the “good” or “connected” state. Locations in which the signal strength is less than this -5 dB threshold are considered to be “blocked” or in the “bad” state.

Measurement locations were chosen to cover many different types of operating environments. Observations of the data suggest appropriate guidelines should be followed in partitioning the data to preserve the stationarity of the statistics.

3.2 QUALITATIVE OBSERVATIONS

Figures 10 through 12 summarize the results from the data collected. The overhead images are derived from MassGIS full-color 0.5 m resolution images taken in April 2001 [14]. Each measurement location is denoted by a colored point plotted on the overhead image. The color corresponds to the signal strength in dB relative to the power received when nothing is blocking the path to the satellite. The latitude and longitude of each measurement location are projected onto the image, which lies in the Massachusetts State Plane.

From the visual depiction of the signal strength, one can immediately see the impact that the density of buildings has on the availability of the communication channel. We see in Figure 10 that street orientation plays a role in the blockages observed. The look angle to the satellite is to the south-southwest. Along streets oriented in this direction, there are almost no blockages. Streets perpendicular to this direction, however, experience frequent blockages. In the close-up image in Figure 10(b), we see that the blockages correspond to specific buildings and are repeatable each time the street is traveled.

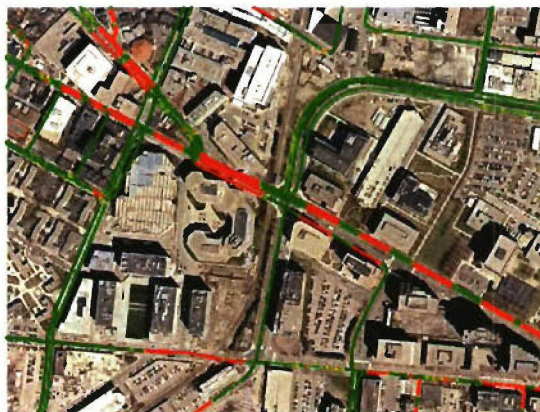
Boston, particularly in the financial district with its higher density of tall buildings, has much larger regions where the signal is unavailable than does Cambridge, which has a lower density of buildings in its layout. The close-up image in Figure 11(b) shows how closely spaced the buildings are in the financial district. In this region, the channel is blocked most of the time, with small opportunities to communicate with the satellite in street intersections or other small gaps between buildings. Regions of Boston outside the financial district, however, are quite similar to the outer regions of residential Cambridge.

The measurements at Devens, MA, are shown in Figure 12. These measurements include vehicle paths over both improved and unimproved roads. The close-up view shown in Figure 12(b) shows the short and rapidly changing blocked and open intervals caused by trees. Both the blocked and open intervals are much shorter in extent than those caused by buildings in urban and suburban environments.

The overall impact on protocol design is as follows: In Boston, upper-layer protocols must adapt to long outages caused by buildings and must be able to take advantage of the relatively few opportunities to transmit and receive data in the open intervals. The effects of foliage are quite different. In these environments, upper-layer protocols must adapt to rapid changes in the blockage state that occur over regions that are much smaller in extent than blocked and open intervals in urban areas.

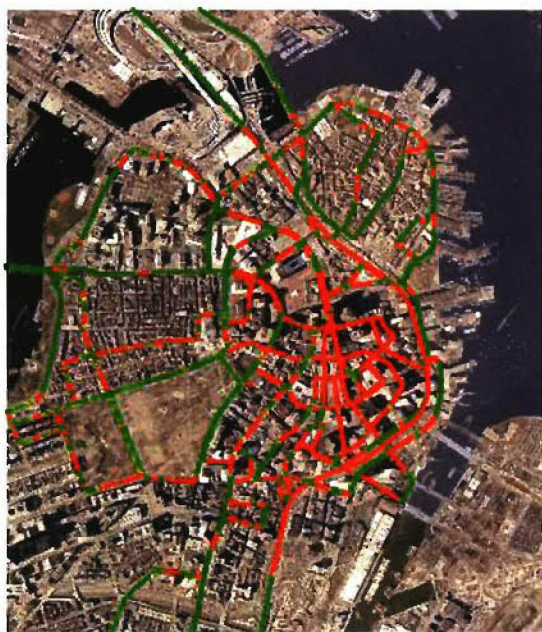


(a) Cambridge, MA

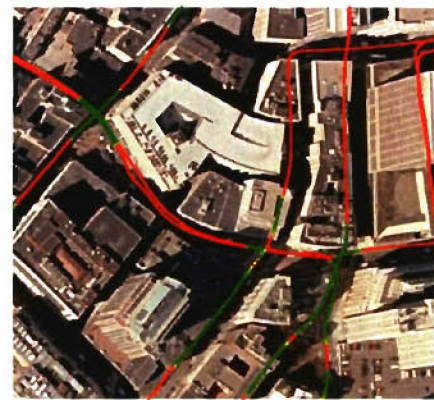


(b) Downtown Cambridge, MA

Figure 10. Signal strength measurements in Cambridge, MA. The measured signal strength is represented using the color scale, shown at right, for each area driven. The signal strength values are given in dB relative to the unobstructed line-of-sight channel.



(a) Boston, MA



(b) Downtown Boston, MA

Figure 11. Signal strength measurements in Boston, MA. The high density of tall buildings results in a high blockage fraction for regions in and around the financial district.

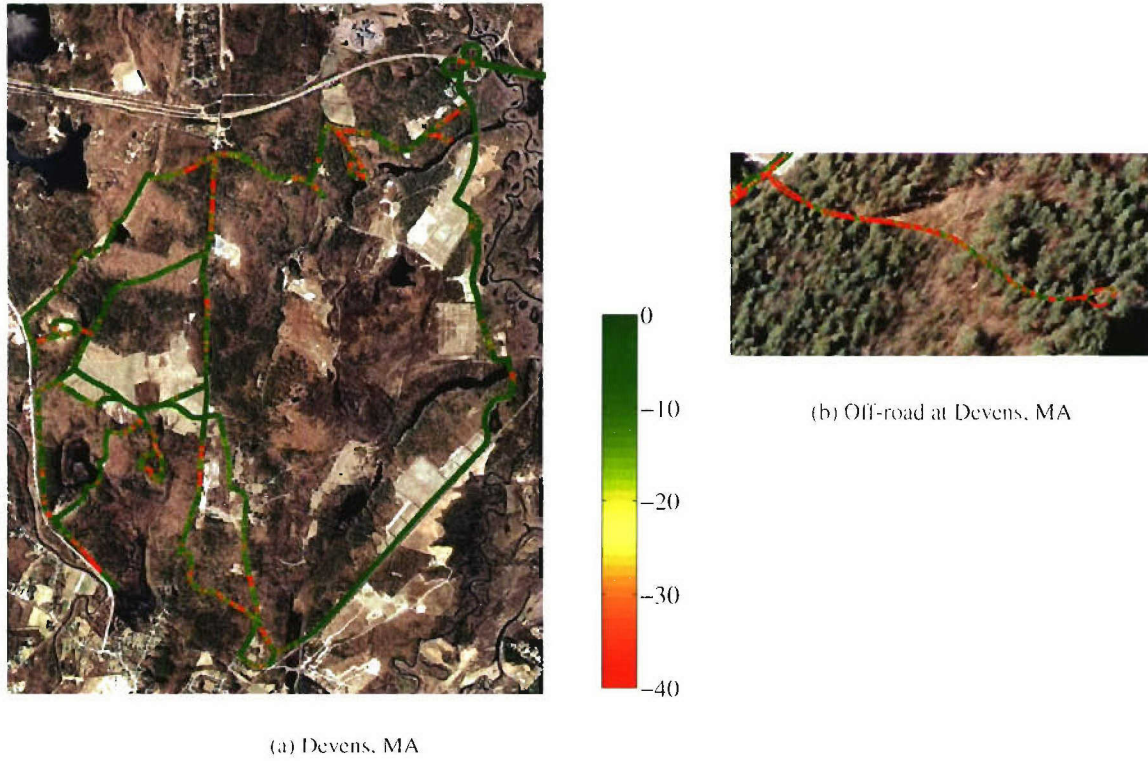


Figure 12. Signal strength measurements in Devens, MA. (a) The experiments at Devens include both improved and unimproved roads. (b) Foliage-induced blockages result in transmit intervals that are very short. Note that the overhead image was taken in the spring and shows more leaves than were present on the trees when the measurements were taken in the fall.

3.3 ANALYSIS

We are interested in the blockage statistics for the new data sets that have been collected. The parameters of interest are blockage fraction and the distribution of blocked and unblocked channel states.

Equidistant spatial samples are used to characterize the fundamental channel behavior based on the environment itself and not the particular velocity profile that was used when making the measurements. We used the spatial data reduction outlined in section 2.4. Time-based samples are converted to distance-based samples using linear power averaging of the time-based samples about each spatial sampling point. Since lower vehicle speeds are used in the city, the urban data sets are sampled more finely than are highway data sets. The spatial sampling intervals used for the data sets in this campaign range from 1.2 m to 3 m.

Figure 13 contains complementary cumulative distribution functions (ccdf's) of the open and blocked durations in various measurement locations. The durations are measured in distance, not in time, so that the results are characteristic of the environment, not particular to the vehicle's velocity profile for a given test. The open durations are distances over which the vehicle continuously maintains connectivity to the satellite. The blocked durations are distances over which the vehicle's path to the satellite is continuously blocked. The results assume a threshold of 5 dB below the received line-of-sight measurement to determine whether the channel is open or blocked.

Clearly, the Boston data set includes longer blockage durations than do the other data sets. This effect is also indicated by the large amount of blocked locations in the financial district as indicated by the red regions in Figure 11. The blockage distributions for Concord, Devens, Cambridge, and the open highway are very similar. In these regions, tree cover, rather than buildings, plays a dominant role in the blockages observed. The composition of the Back Bay falls in between that of Boston and Cambridge, and the blockage distribution reflects this mixture of buildings and trees.

Not surprisingly, the open highway data set includes very long open intervals. These open intervals are interrupted only by the occasional bridge or grove of trees that obstructs the path to the satellite. The contrast between natural and man-made obstructions is also evident in Figure 13(b). Regions where the blockage is dominated by tree cover present short but frequent opportunities to communicate. The connection durations are longer, on average, in Boston and Cambridge than they are for Devens or the Concord Loop, where tree cover is more prominent.

Table 3 summarizes the statistics for data sets gathered in each measurement region. The values for Boston include the entire Boston data set. When restricted to just the financial district, however, the blockage fraction rises to 89%. The blockage fractions for urban areas and for the open highway are consistent with values reported by Lutz, *et al.* [15].

3.4 GUIDELINES FOR PARTITIONING DATA SETS

The Lincoln Laboratory data that was collected in 2002 included repetitions of a single loop around Cambridge [1]. Given the tracking capabilities of a newer terminal, data sets of much longer durations were collected in Cambridge during the 2004 measurement campaign. The statistics of the larger data set are compared to only the route taken in the 2002 campaign. Figure 14 shows the blocked and open distributions for the two sets of data. The 2002 route includes long portions of roadway along the Charles River, where

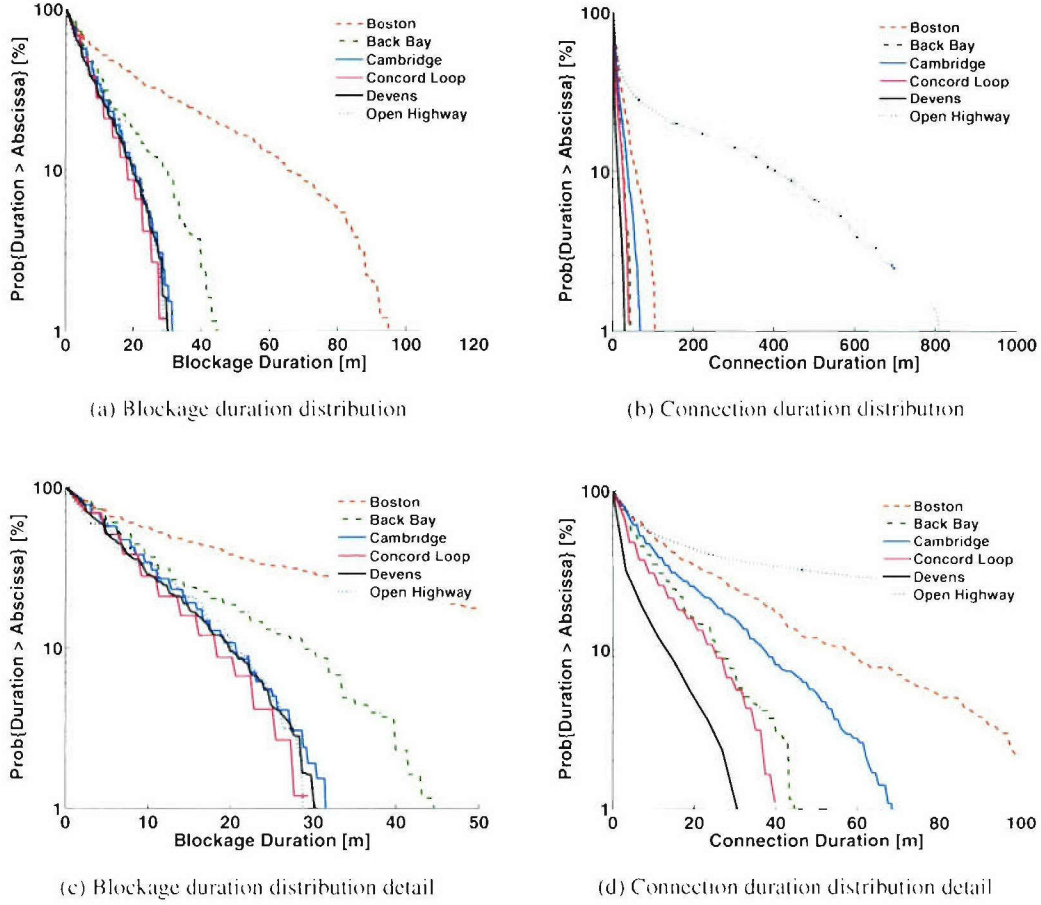


Figure 13. Summary distributions of blocked and open intervals. The plots in (a) and (b) show the distribution of blocked and unblocked spatial intervals for each measurement area. The plots in (c) and (d) zoom in on the x-axis for the plots above.

the path to the satellite remains unblocked. As a result, the distribution of open intervals for the 2002 data set indicates intervals that are much longer than are characteristic for Cambridge as a whole.

Similarly, the data set that describes Boston consists of two very different regions. The city center contains a dense urban core of tall, closely spaced buildings. Outside this core are areas with lower building densities and more vegetation. Due to the high density of tall buildings in the financial district, the distributions for the data in this region are different from the distributions for the entire city, as reflected in Figure 15.

TABLE 3
Summary of Blockage Statistics

Location	Blockage Fraction	Mean Blockage	Mean Open
Boston	46%	44 m	51 m
Boston (<i>fin. dist. only</i>)	89%	130 m	18 m
Back Bay	49%	21 m	21 m
Cambridge	32%	15 m	30 m
Cambridge Subset	21%	16 m	60 m
Concord Loop	42%	15 m	20 m
Devens	35%	15 m	28 m
Open Highway	5%	17 m	310 m

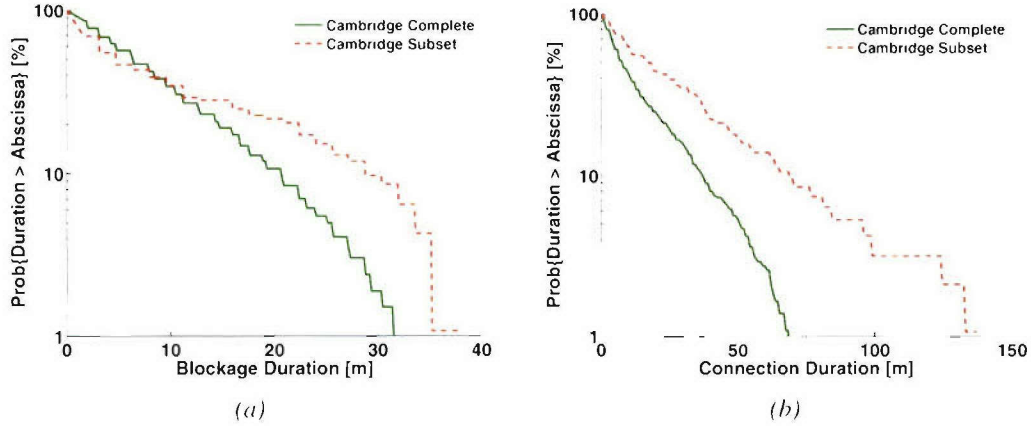


Figure 14. Distributions of blocked and open intervals for Cambridge data sets. The smaller subset of data taken in 2002 has a distribution of longer blockage intervals. The larger Cambridge data set contains connection durations that are shorter, on average, than those of the 2002 data set.

Since there is a strong connection between terrain features and channel impairments, a logical grouping of data sets accounts for terrain features in the environment. Schodorf [1] recognizes this fact and groups environments into three broad categories: urban, rural, and open.

The analysis presented in this section, however, suggests that a further subdivision of the urban environment may be necessary. Using urban planning data to group neighborhoods by common building types within a city can be useful for selecting regions with consistent blockage statistics. The smaller clusters of homogeneous terrain regions can be grouped together in a larger model that transitions between regions at larger time constants, reflecting the meandering of a vehicle from one region to another.

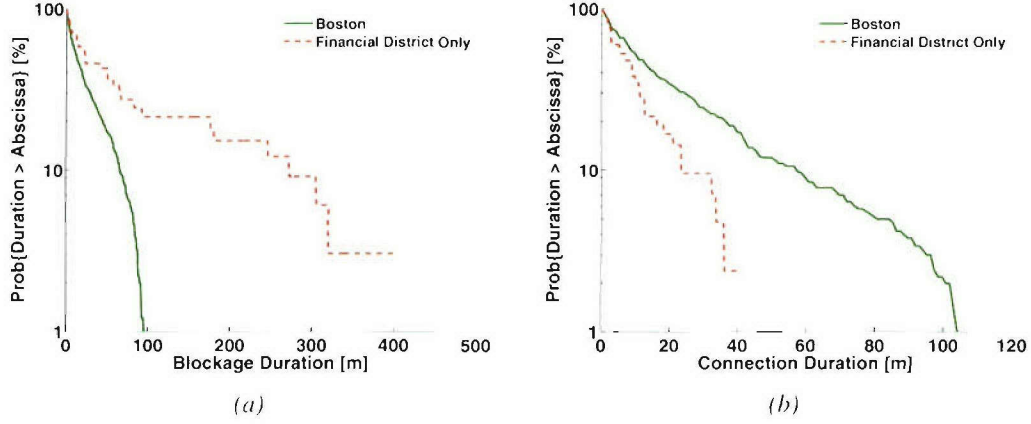


Figure 15. Distributions of blocked and open intervals for Boston data sets. The blocked intervals (a) in the financial district are much longer, on average, than the average blockage interval for the entire Boston data set. The open intervals in the financial district are much shorter, on average, than the average open interval for the entire Boston data set.

3.5 PARAMETERS FOR MARKOV MODELS

The behavior of the SATCOM on-the-move channel is frequently modeled by Markov processes [11, 12, 1, 13], the simplest of which is shown in Figure 16. The modeling can be done in either the temporal or the spatial domain. The model consists of two states. The “good” state **g** represents times or locations over which the terminal is not blocked by physical obstructions, and communication with the satellite can occur error free. The “bad” state **b** represents times or locations over which the terminal is blocked by obstructions, and no communication occurs with the satellite. Transition probabilities at each time or distance sampling point are labeled along the arcs representing the state transitions.

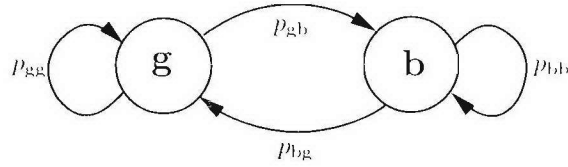


Figure 16. The two-state Markov model. The simple two-state models represents two states, a “good” state **g** denoting error-free communication and a “bad” state **b** in which communication is lost.

The ccdl’s of the open and blocked durations are given as [1]

$$\Pr\{D_b > n\} = p_{bb}^n \quad (1)$$

$$\Pr\{D_g > n\} = p_{gg}'' \quad (2)$$

where D_b and D_g are the number of continuous samples for which the channel remains in the good or bad state.

The two-state Markov model has two degrees of freedom and is completely specified by any two of the four transition probabilities. The cdf's for all measurement regions are shown in Figure 17. By matching (1) and (2) for both blocked and connected durations, we can specify the model for each region. These results are summarized in Table 4. The values for blockage fraction, π_b , are computed from p_{bb} and p_{gg} using the following relationships given by [1]:

$$\begin{aligned} \pi_b &= \frac{p_{gb}}{p_{gb} + p_{bg}} \\ p_{gb} &= 1 - p_{gg} \\ p_{bg} &= 1 - p_{bb} \end{aligned} \quad (3)$$

The values for p_{bb} and p_{gg} correspond to the dashed green line in the plots in Figure 17.

For many of the measurement regions, there is a “dip” in the distribution function for connection duration. An extra degree of freedom in the blockage model is required to fit the L-shaped curve in these cases. The Gilbert model used by [1] decouples the state of the underlying model from the observed state. In particular, the good state denotes error-free communication, and the “bad” state has a probability h of having error-free communication for the specified sampling period. In this case, the complementary cdf's are given by [1]

$$\begin{aligned} \Pr\{D_\gamma > n\} &= Ag_1'' + (1 - A)g_2'' \\ \Pr\{D_\beta > n\} &= (1 - h)''p_{bb}'' \end{aligned} \quad (4)$$

where D_γ and D_β are the number of continuous samples for which the channel observations are consistent with error-free (*i.e.*, “good” observations) communications or channel errors (*i.e.*, “bad” observations), respectively. The parameters A , g_1 , and g_2 are intermediate parameters and are related to state transition probabilities and the “bad” state observation probability, h , as follows:

$$\begin{aligned} h &= \frac{g_1 g_2}{g_1 - A(g_1 - g_2)} \\ p_{gb} &= \frac{(1 - g_1)(1 - g_2)}{1 - h} \\ p_{bg} &= A(g_1 - g_2) + (1 - g_1) \left(\frac{g_2 - h}{1 - h} \right) \end{aligned} \quad (5)$$

This added degree of freedom in the model permits us to fit the data to two piecewise linear segments, on a semi-log scale, to the connection duration distributions of Figure 17. Using this method, the Gilbert model fits the connection distribution quite well. The red dotted lines in Figure 17 correspond to the Gilbert model parameters listed in Table 5. While the connection duration distribution matches quite well, the

TABLE 4
Parameters Using the Two-State Markov Model

Location	p_{gg}	p_{bb}	π_b
Boston	0.9919	0.9866	0.38
Boston (<i>fin. dist. only</i>)	0.9502	0.9941	0.89
Back Bay	0.9806	0.9730	0.42
Cambridge	0.9885	0.9564	0.21
Cambridge Subset	0.9898	0.9479	0.16
Concord Loop	0.9819	0.9702	0.38
Devens	0.9954	0.9691	0.13
Open Highway	0.9988	0.9779	0.05

TABLE 5
Parameters Using the Gilbert Model with Connection Duration Only

Location	p_{gg}	p_{bb}	h	π_A	A	g_1	g_2
Boston	0.9940	0.9685	0.8568	0.023	0.804	0.8288	0.9949
Boston (<i>fin. dist. only</i>)	0.9412	0.4935	0.4156	0.061	0.320	0.1887	0.9576
Back Bay	0.9864	0.9576	0.7550	0.060	0.165	0.9880	0.7213
Cambridge	0.9742	0.8318	0.8830	0.016	0.321	0.7195	0.9892
Cambridge Subset	0.9934	0.9912	0.9622	0.016	0.760	0.9524	0.9947
Concord Loop	0.9876	0.9551	0.6692	0.072	0.869	0.6381	0.9886
Devens	0.9980	0.9953	0.8332	0.049	0.972	0.8293	0.9981
Open Highway	0.9990	0.9961	0.9847	0.003	0.780	0.9806	0.9992

blocked distribution does not match at all when fitting the data to only the connection duration distribution using the Gilbert model. This, too, was observed by [1].

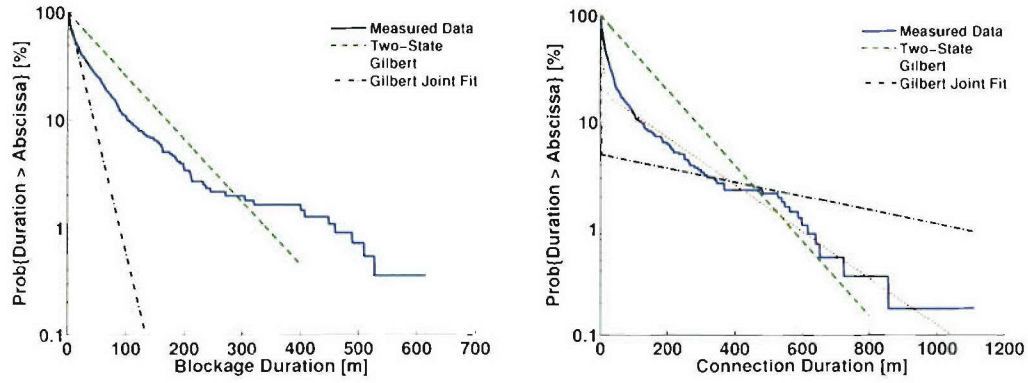
From the red dotted lines in Figure 17, we see that a very good fit can be achieved if all three parameters can be varied to fit the connection duration cdf. Schodorf [1] fits the Gilbert model to both open and blocked duration cdf's to achieve a better overall fit than when using the two-state model. This approach essentially trades accuracy in the connection duration cdf for improved accuracy in the blockage duration cdf. A reasonable fit can be attained if the average blockage duration is not too great. When the average blockage duration is too large, however, one of the free parameters must be made so small that a degree of freedom is essentially lost. We see an instance of this in [1] as the parameter h must be made very small for cases with the largest average blockage duration. Making h very small has the effect of concentrating most of the connection duration distribution before the breakpoint, which in some cases produces a poor fit.

TABLE 6

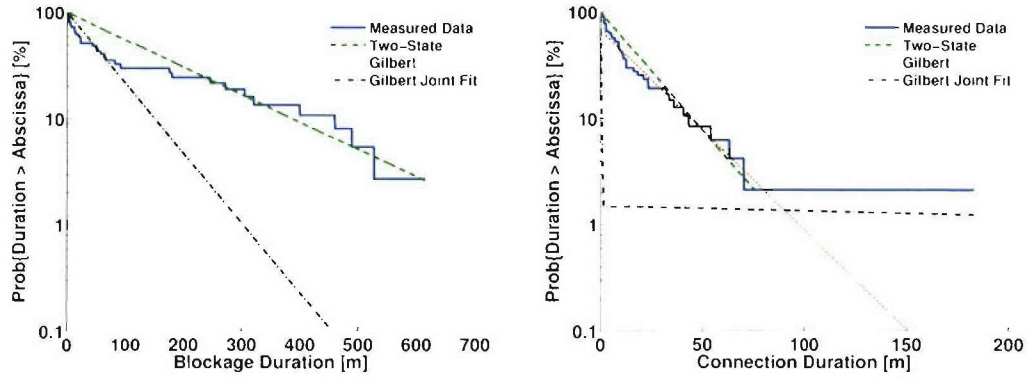
Parameters Using the Gilbert Model, Jointly Fitting Blockage and Connection Durations

Location	p_{gg}	p_{bb}	h	π_{β}	A	g_1	g_2
Boston	0.9985	0.9501	1.053×10^{-4}	0.029	0.050	0.9985	1.000×10^{-4}
Boston (<i>fin. dist. only</i>)	0.9990	0.9850	1.015×10^{-4}	0.063	0.015	0.9990	1.000×10^{-4}
Back Bay	0.9950	0.9155	0.0005	0.056	0.085	0.9950	0.0005
Cambridge	0.9945	0.9433	1.060×10^{-4}	0.088	0.057	0.9945	1.000×10^{-4}
Cambridge Subset	0.9987	0.9451	1.058×10^{-4}	0.023	0.055	0.9987	1.000×10^{-4}
Concord Loop	0.9920	0.9405	1.064×10^{-4}	0.118	0.060	0.9920	1.000×10^{-4}
Devens	0.9975	0.9601	0.0010	0.059	0.040	0.9975	0.0010
Open Highway	0.9995	0.9151	1.093×10^{-4}	0.006	0.085	0.9995	1.000×10^{-4}

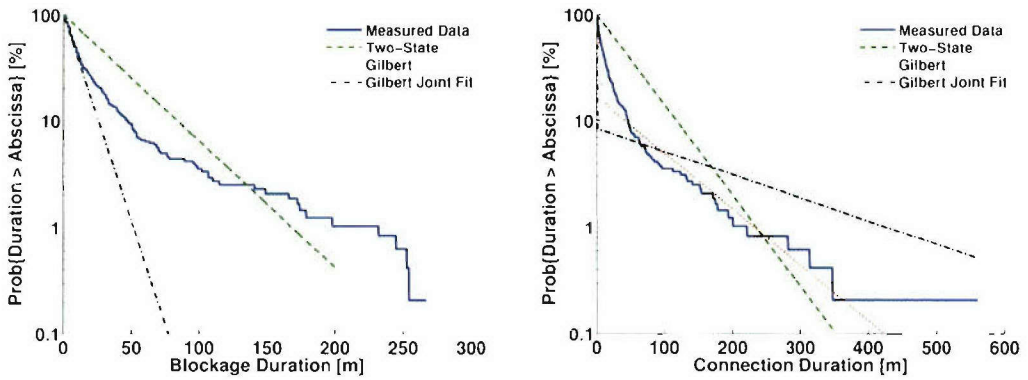
The black dash-dot lines in Figure 17 correspond to the values in Table 6. These parameters were chosen to make the best fit to both blockage and connection duration cdf's. We again observe that the quality of the fit using the Gilbert model depends on the relative sizes of the blockage and connection durations. We see that the best fits occur in Figures 17(d)–(g), where the blockage durations are significantly less than the connection durations. Figures 17(a)–(c) are examples in which the blockage durations are the same size or larger than the connection durations. In these cases, the data does not agree as well with the Gilbert model.



(a) Boston

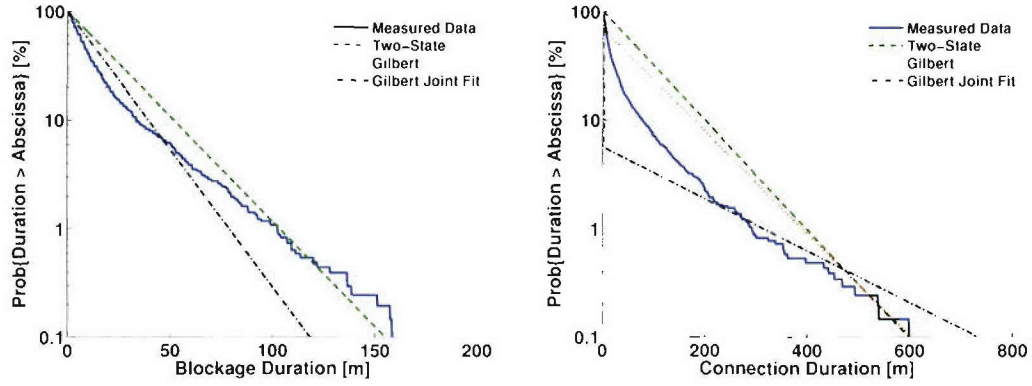


(b) Boston Financial District

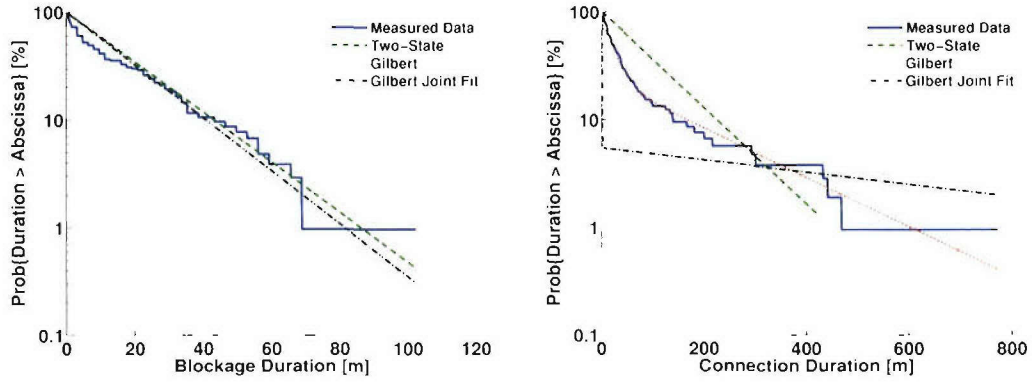


(c) Back Bay

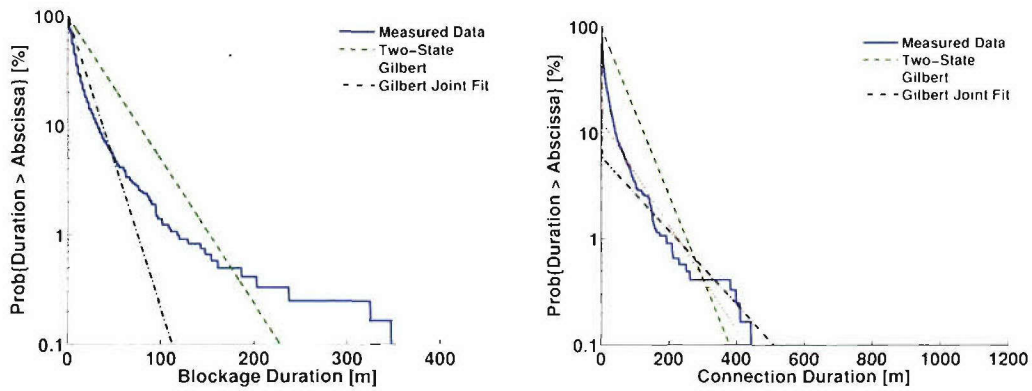
Figure 17. Parameter matching for Markov channel state models. The two-state model provides a good match for the data obtained in the Boston financial district. In the other areas, the Gilbert model matches the connection duration well but does not simultaneously model the blockage duration distributions.



(d) Cambridge

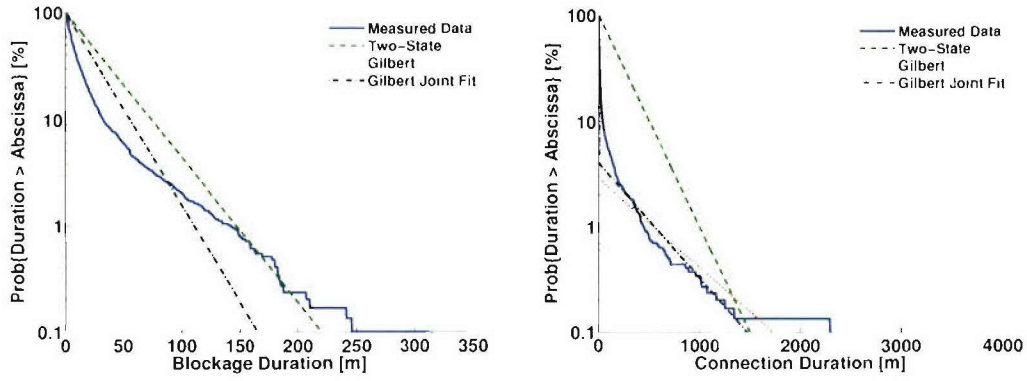


(e) Cambridge Subset

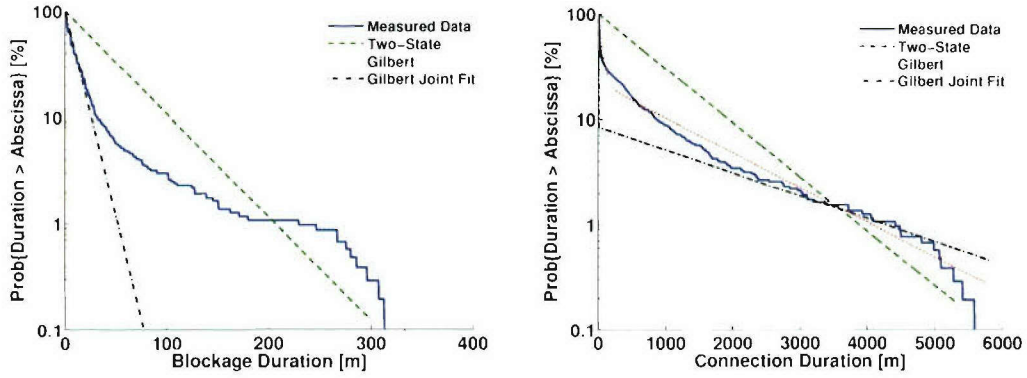


(f) Concord Loop

Figure 17. Parameter matching for Markov channel state models (continued).



(g) Devens, MA



(h) Open Highway

Figure 17. Parameter matching for Markov channel state models (continued).

3.6 SUMMARY

With its improved stability, the second SATCOM on-the-move prototype vehicle developed at Lincoln Laboratory was used to conduct an extensive measurement campaign in and around Boston, MA. In this chapter, we present the results of this campaign. The primary difference between the data presented here and the data presented in [1] is that we included more measurement environments and that individual experiments tended to be longer in duration, resulting in data sets that are more representative of the given regions.

After making some qualitative observations that led to a natural partitioning of the data sets, we proposed two new regions to describe probable operating environments for SATCOM on-the-move systems: open highway and dense urban.

The new data sets gathered in this measurement campaign cover larger geographical areas than those of the previous campaign [1], resulting in a drastically increased volume of data. We confirmed many of the observations of [1, 13] using the new data sets. Although there are clearly deficiencies in the two-state model, it can easily be specified over a wide range of parameters. The jointly fit Gilbert model used by [1] can provide a better fit to the data in certain circumstances, it is still unclear how generally applicable the model is to a wide range of environments, particularly those with longer blockage durations.

4. MULTIPLE-TERMINAL TECHNIQUES

We learn from Chapter 3 that blockage is a problem for SATCOM on-the-move ground terminals and can become quite severe, especially in urban areas. Since blockage is a physical phenomenon, we look for system designs that can mitigate the blockage effects. It is well known for terrestrial communications that link diversity may be used to improve link quality for a channel with fast fading [16]. We apply this same general idea to SATCOM on the move by using multiple nodes in a cooperative manner to improve utilization of the SATCOM link.

In this chapter, we explore the fundamental limits of techniques using multiple, cooperative ground terminals. In section 4.1 we follow the derivation of Yao [17] for blockage behavior when multiple terminals are used. We compare theory to measurements for this behavior. Cooperative nodes are expected to achieve better combined performance if their link states are not highly correlated with each other. Section 4.2 presents correlation properties of two cooperative nodes, both of which experience blockage. Measurements from different operating environments are presented in section 4.3 to compare correlation properties with theoretical predictions.

4.1 BLOCKAGE PROPERTIES FOR MULTIPLE COOPERATING GROUND TERMINALS

In this section, we summarize the derivation of the blocking probabilities and the mean open and blocked durations derived by Yao [17]. We consider the blocking probability of a system with N cooperating ground terminals. Assuming perfect cooperation among all the ground terminals, the channel is effectively blocked only when all N terminals are simultaneously blocked. In other words, cooperation allows all terminals to access the satellite as long as at least one terminal has good SATCOM connectivity.

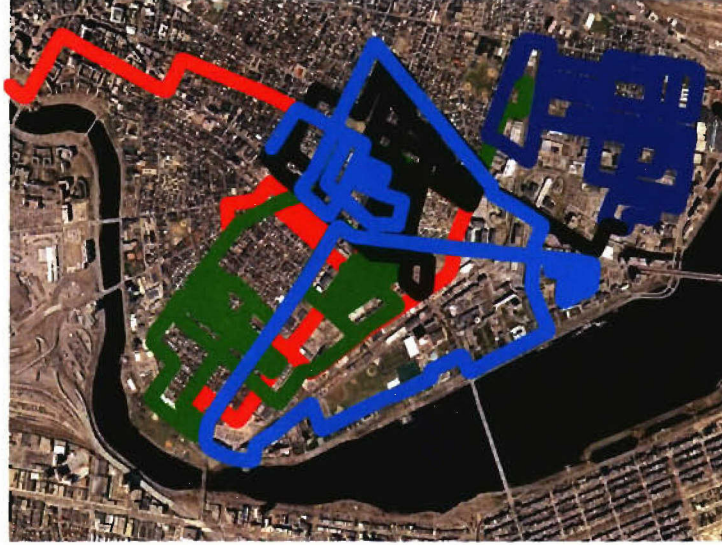
Since the cluster of ground terminals are operating in the same general area, we assume that all N terminals have identical blockage statistics. If the terminals experience independent blockages, the blocking probability for all N terminals is then

$$\pi_{b,N} = \pi_b^N. \quad (6)$$

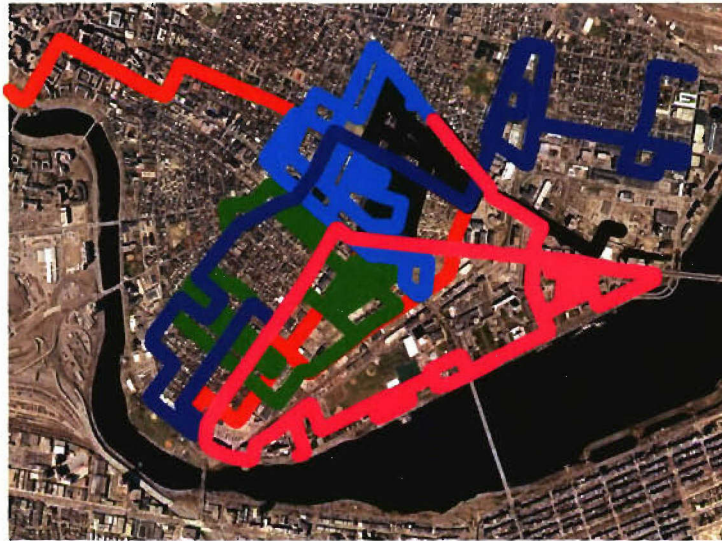
where π_b is the blocking probability for an individual ground node. The probability that the entire ground cluster has some SATCOM connectivity is

$$\pi_{g,N} = 1 - \pi_{b,N} = 1 - \pi_b^N. \quad (7)$$

To evaluate (6) and (7) with experimental data, we are faced with the choice of performing the analysis in the spatial domain or in the time domain. Spatial domain analysis is attractive because the results are applicable to the environment and not the velocity profile of the measurement vehicle. Time-domain analysis is appealing, however, since all signal processing techniques eventually need to be performed in the time domain.



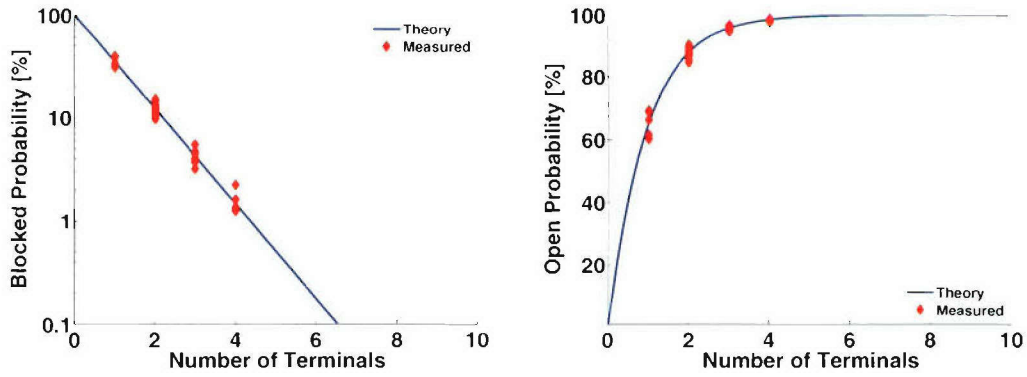
(a) Spatial domain routes



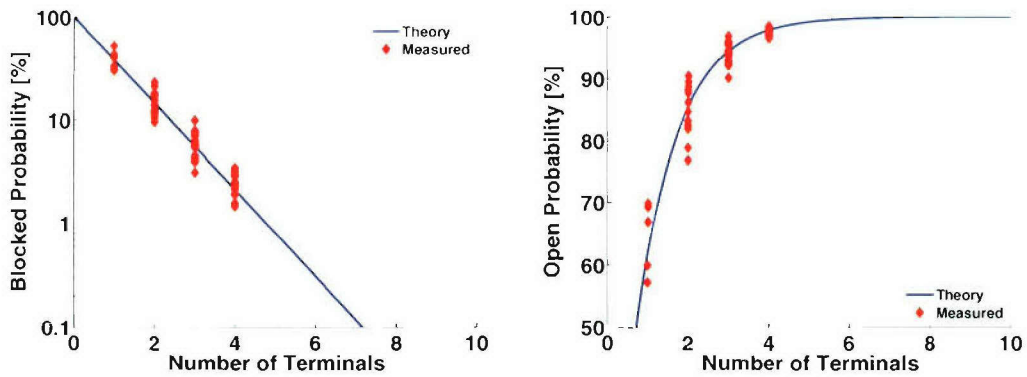
(b) Time domain routes

Figure 18. Independent routes used for spatial and time domain analyses. The portions of the routes used for different theoretical ground terminals are shown in different colors.

In this section, we analyze the results for both spatial and time domains. The spatial domain data is derived from the time series data as described in section 2.4. Since equations (6) and (7) assume independent blocking across the nodes, we break up the drive path for the Cambridge data set into segments that are 12-km long for the spatial analysis and 30-minutes long for time domain analysis. The drive routes for each of these segments are shown in Figure 18. When these segments are processed in parallel, each route is used to emulate one node in a cooperative cluster. Because the routes are scattered, each node effectively experiences independent channel blockage.



(a) Spatial domain analysis



(b) Time domain analysis

Figure 19. Blockage and connection probabilities of scattered cooperating terminals using spatial and time domain analyses. The agreement between theory and measurement in these plots is fundamentally a result of the statistical independence of the states observed for each terminal.

Figure 19 shows empirical blocking probabilities compared to the theoretical predictions of (6) and (7). The empirical probabilities are computed by counting the number of good or bad states in the data segment and dividing by the total number of samples in that segment. When multiple cooperating nodes are considered, a time or spatial state sample is considered bad only when all nodes are simultaneously blocked and good otherwise.

From Figure 19 we see very good agreement with the theoretical predictions since care was taken to make the channel blockages appear to be independent among the nodes. When the nodes are in convoy, however, this independence assumption is no longer valid.

Next, we consider convoy scenarios in which we vary the inter-vehicle spacing to show the changes that occur when the channel become more or becomes less correlated between vehicles. For this analysis, we consider a single data set from Cambridge that is three hours long and covers approximately 40 km of linear distance traveled. For the spatial analysis, convoy vehicles maintain a constant inter-vehicle spacing of 30 m. For the time-domain analysis, all vehicles follow the same trajectory, including the same variations in vehicle speed. Each vehicle is delayed by 20, 50, or 100 seconds from the previous vehicle.

The results of the cooperative blocked and open probabilities are shown in Figure 20. As the vehicles in the convoy become more closely spaced, the performance degrades relative to the performance for independent blockages.

We now consider the mean blocked and open durations of a cooperating cluster of ground terminals. We define T_g as the average dwell time in the good state and T_b as the average dwell time in the bad state of a two-state Markov process. We can write the state transition probabilities in terms of a time step τ [17]:

$$\begin{aligned} p_{gb} &= \pi_b \left(1 - e^{-\tau/T_0} \right) \\ p_{bg} &= \pi_g \left(1 - e^{-\tau/T_0} \right), \end{aligned} \quad (8)$$

where

$$T_0 = \frac{T_g T_b}{T_g + T_b}. \quad (9)$$

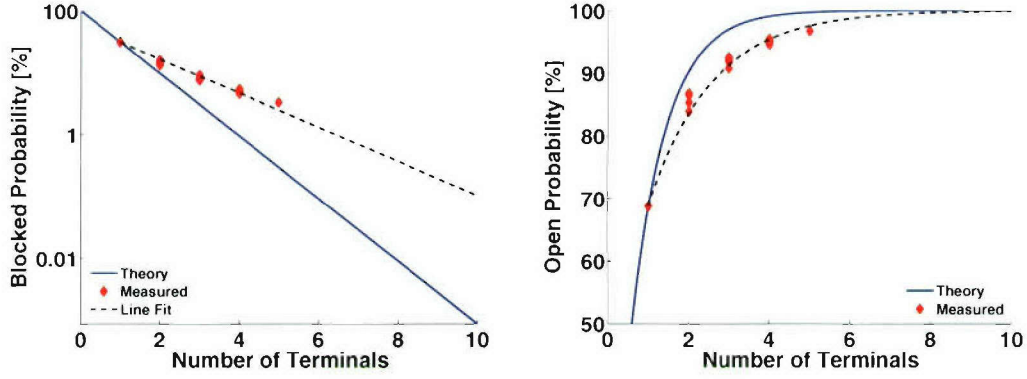
When $\tau \ll T_0$, (8) can be re-written as

$$\begin{aligned} p_{gb} &\approx \frac{\tau}{T_g} \\ p_{bg} &\approx \frac{\tau}{T_b} \end{aligned} \quad (10)$$

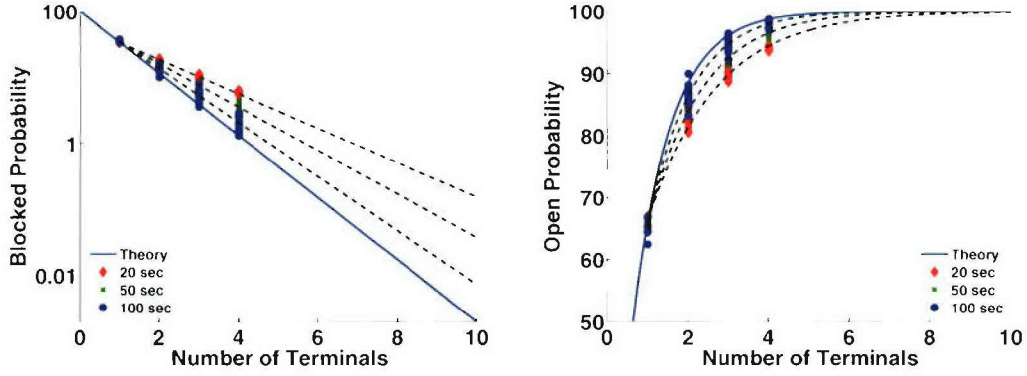
For a cluster of N cooperating nodes, an equivalent two-state Markov chain can be constructed in which the bad state corresponds to all N links from the cluster to the satellite being blocked. The equivalent expression for T_b in (10) is [17]

$$T_{b,N} \approx \frac{\tau}{p_{bg,N}} = \frac{\tau}{1 - p_{bb,N}} = \frac{\tau}{1 - p_{bb}^N} = \frac{\tau}{1 - (1 - p_{bg})^N} \approx \frac{\tau}{N p_{bg}} \approx \frac{T_b}{N}. \quad (11)$$

where the second approximation comes from the assumption that $p_{bg} \ll 1$ and the third approximation is from a substitution for T_b according to (10).



(a) Constant spatial separation of 30 m



(b) Constant time separation

Figure 20. Blockage and connection duration probabilities of cooperating terminals in convoy with (a) constant speed and fixed-distance separation between vehicles and (b) variable speed and fixed time separation between vehicles. As the convoy vehicles are more closely spaced, the observed states become more correlated with each other and the observed blockage and connection probabilities deviate from the theoretical predictions.

Using the ergodic relationship between dwell times and state probabilities,

$$\frac{T_{g,N}}{T_{b,N}} = \frac{p_{g,N}}{p_{b,N}}. \quad (12)$$

we get a relationship for dwell time in the good state [17]:

$$T_{g,N} = \left(\frac{T_b}{N} \right) \left(\frac{1 - p_b^N}{p_b^N} \right) \quad (13)$$

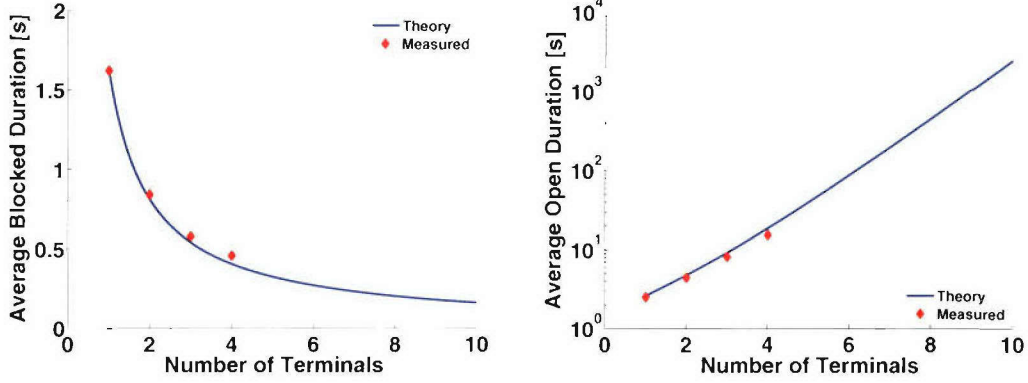


Figure 21. Average blocked and open durations for scattered cooperating nodes. In this case, the state observations are statistically independent between ground terminals and the corresponding measurements agree well with the theory.

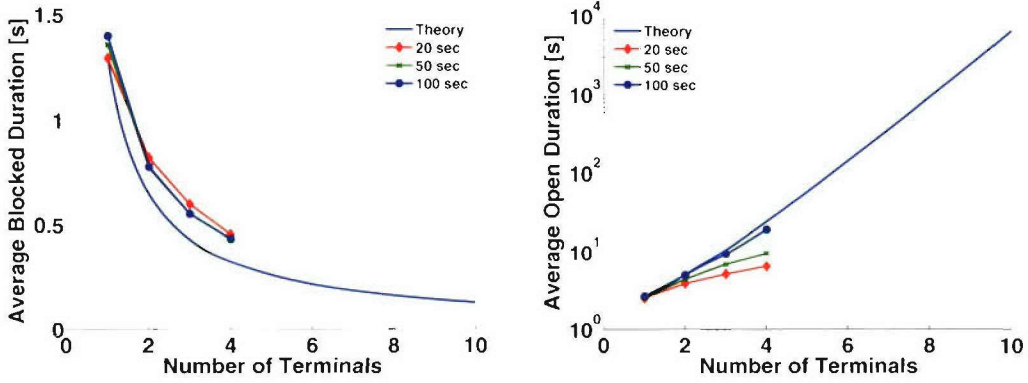


Figure 22. Average blocked and open durations for cooperating nodes in convoy. As the correlation among observed states increases, the marginal benefit of an additional terminal is less than what the theory predicts.

Although the previous derivation can be done for the spatial domain using a distance variable rather than a time variable, we limit our comparison with the experimental data to the time domain case. The equations of interest are (11) and (13). Figure 21 shows the results for the case in which the nodes are scattered as in Figure 18. Because of the independent blockages and the fact that the approximations in the preceding derivation hold, the measurements agree quite well with the theoretical predictions. For the case of more correlated channel blockages in a convoy scenario, we see in Figure 22 that the performance deviates from the independent blockage case as the convoy nodes are more closely spaced.

4.2 AUTOCORRELATION PROPERTIES OF A TWO-STATE MARKOV PROCESS

In this section, we derive the correlation coefficient of a Markov process. Since the correlation coefficient is a quantitative measure of the output of the Markov state, each state must be associated with a numeric output value. We generalize the approach taken by [18] to an N -state Markov process with arbitrary values for the state outputs. The state outputs are numerical values corresponding to each Markov state. These values are used to compute the correlation coefficient of a particular Markov model. Let $s = [s_1 \ s_2 \ \cdots \ s_N]$ be the vector representing the output values of each of the N Markov states.

Let X_i be a random variable indicating the state of the Markov process at time i . We say $X_i = s_j$ when the process is in state j at time i .

Let

$$\mathbf{M} = \begin{bmatrix} \Pr\{X_{i+1} = s_1 | X_i = s_1\} & \Pr\{X_{i+1} = s_2 | X_i = s_1\} & \cdots & \Pr\{X_{i+1} = s_N | X_i = s_1\} \\ \Pr\{X_{i+1} = s_1 | X_i = s_2\} & \Pr\{X_{i+1} = s_2 | X_i = s_2\} & \cdots & \Pr\{X_{i+1} = s_N | X_i = s_2\} \\ \vdots & \vdots & \ddots & \vdots \\ \Pr\{X_{i+1} = s_1 | X_i = s_N\} & \Pr\{X_{i+1} = s_2 | X_i = s_N\} & \cdots & \Pr\{X_{i+1} = s_N | X_i = s_N\} \end{bmatrix} \quad (14)$$

be the transition probabilities between the states in the model.

Let $\pi = [\pi_1 \ \pi_2 \ \cdots \ \pi_N]$ be the steady state probabilities of being in any of the N states. The steady state solutions are found by solving the following system of equations:

$$\begin{aligned} \mathbf{M}\pi &= \pi \\ \pi^T \mathbf{1} &= 1, \end{aligned} \quad (15)$$

where $\mathbf{1}$ is the vector of all ones.

After n time steps, n successive applications of the \mathbf{M} matrix give the marginal probabilities of transitioning between each of the states:

$$\mathbf{M}^n = \begin{bmatrix} \Pr\{X_{i+n} = s_1 | X_i = s_1\} & \Pr\{X_{i+n} = s_2 | X_i = s_1\} & \cdots & \Pr\{X_{i+n} = s_N | X_i = s_1\} \\ \Pr\{X_{i+n} = s_1 | X_i = s_2\} & \Pr\{X_{i+n} = s_2 | X_i = s_2\} & \cdots & \Pr\{X_{i+n} = s_N | X_i = s_2\} \\ \vdots & \vdots & \ddots & \vdots \\ \Pr\{X_{i+n} = s_1 | X_i = s_N\} & \Pr\{X_{i+n} = s_2 | X_i = s_N\} & \cdots & \Pr\{X_{i+n} = s_N | X_i = s_N\} \end{bmatrix}. \quad (16)$$

Within this framework, we find the correlation coefficient of the process. We define the correlation coefficient of the random process consisting of the Markov state output values as [19]

$$R[n] = \frac{\mathbb{E}[(X_{i+n} - \mathbb{E}[X_{i+n}]) (X_i - \mathbb{E}[X_i])]}{\sqrt{\text{Var}[X_{i+n}]} \sqrt{\text{Var}[X_i]}} \quad (17)$$

We assume the process is stationary and that

$$\begin{aligned} \mathbb{E}[X_{i+n}] &= \mathbb{E}[X_i] \triangleq \mathbb{E}[X] \\ \text{Var}[X_{i+n}] &= \text{Var}[X_i] \triangleq \text{Var}[X]. \end{aligned} \quad (18)$$

The correlation coefficient becomes

$$\begin{aligned}
R[n] &= \frac{\mathbb{E}[(X_{i+n} - \mathbb{E}[X_{i+n}])(X_i - \mathbb{E}[X_i])]}{\text{Var}[X]} \\
&= \frac{\mathbb{E}[X_{i+n}X_i] - \mathbb{E}[X]^2}{\mathbb{E}[X^2] - \mathbb{E}[X]^2} \\
&= \frac{\mathbb{E}[X_{i+n}X_i] - \mathbb{E}[X]^2}{\mathbb{E}[X^2] - \mathbb{E}[X]^2}.
\end{aligned} \tag{19}$$

Below, we find expressions for each of the expectations in (19):

$$\begin{aligned}
\mathbb{E}[X] &= \sum_{j=1}^N s_j \Pr\{X = s_j\} = \sum_{j=1}^N s_j \pi_j \\
&= \boldsymbol{\pi}^T \mathbf{s},
\end{aligned} \tag{20}$$

$$\mathbb{E}[X^2] = \sum_{j=1}^N s_j^2 \pi_j = \boldsymbol{\pi}^T \mathbf{s}_2, \tag{21}$$

where $\mathbf{s}_2 = [s_1^2 \ s_2^2 \ \dots \ s_N^2]^T$, and

$$\begin{aligned}
\mathbb{E}[X_{i+n}X_i] &= \sum_{j=1}^N \sum_{k=1}^N s_j s_k \Pr\{X_{i+n} = s_j, X_i = s_k\} \\
&= \sum_{j=1}^N s_j \sum_{k=1}^N s_k \Pr\{X_{i+n} = s_j | X_i = s_k\} \Pr\{X_i = s_k\} \\
&= \sum_{j=1}^N s_j \sum_{k=1}^N s_k \pi_k \Pr\{X_{i+n} = s_j | X_i = s_k\} \\
&= \mathbf{s}_\pi^T \mathbf{M}^n \mathbf{s},
\end{aligned} \tag{22}$$

where $\mathbf{s}_\pi = [s_1 \pi_1 \ s_2 \pi_2 \ \dots \ s_N \pi_N]^T$. Substituting (20)–(22) into (19), we get

$$R[n] = \frac{\mathbf{s}_\pi^T \mathbf{M}^n \mathbf{s} - (\boldsymbol{\pi}^T \mathbf{s})^2}{\boldsymbol{\pi}^T \mathbf{s}_2 - (\boldsymbol{\pi}^T \mathbf{s})^2} \tag{23}$$

For the two-state Markov process, we have the transition probability matrix

$$\mathbf{M} = \begin{bmatrix} p_{bb} & p_{bg} \\ p_{gb} & p_{gg} \end{bmatrix}. \tag{24}$$

From Schodorf and Wu [18], we can write \mathbf{M}^n for the two-state model as follows:

$$\mathbf{M}^n = \begin{bmatrix} \pi_g \alpha^n + \pi_b & -\pi_g \alpha^n + \pi_g \\ -\pi_b \alpha^n + \pi_b & \pi_b \alpha^n + \pi_g \end{bmatrix}. \tag{25}$$

The parameter α is found by setting the elements of (25) to those of (24). We find

$$\alpha = \frac{p_{gg} - \pi_g}{\pi_b} = \frac{p_{bb} - \pi_b}{\pi_g}. \quad (26)$$

We compute the correlation coefficient for the two-state Markov model with arbitrary state outputs $\mathbf{s} = \begin{bmatrix} s_b & s_g \end{bmatrix}$. The correlation coefficient is

$$\begin{aligned} R[n] &= \frac{\begin{bmatrix} s_b \pi_b & s_g \pi_g \end{bmatrix} \begin{bmatrix} \pi_g \alpha^n + \pi_b & -\pi_g \alpha^n + \pi_g \\ -\pi_b \alpha^n + \pi_b & \pi_b \alpha^n + \pi_g \end{bmatrix} - \left(\begin{bmatrix} \pi_b & \pi_g \end{bmatrix} \begin{bmatrix} s_b \\ s_g \end{bmatrix} \right)^2}{\begin{bmatrix} \pi_b & \pi_g \end{bmatrix} \begin{bmatrix} s_b^2 \\ s_g^2 \end{bmatrix} - \left(\begin{bmatrix} \pi_b & \pi_g \end{bmatrix} \begin{bmatrix} s_b \\ s_g \end{bmatrix} \right)^2} \\ &= \frac{\pi_b \pi_g (s_b - s_g)^2 \alpha^n}{s_b^2 \pi_b (1 - \pi_b)^2 - 2 s_b s_g \pi_b \pi_g + s_g^2 \pi_g (1 - \pi_g)}. \end{aligned} \quad (27)$$

Using the fact that $\pi_b + \pi_g = 1$, we find that the correlation coefficient for the two-state Markov process is exponential, regardless of the choice of state output values:

$$R[n] = \frac{\pi_b \pi_g (s_b - s_g)^2 \alpha^n}{\pi_b \pi_g (s_b - s_g)^2} = \alpha^n. \quad (28)$$

4.3 EMPIRICAL RESULTS FOR AUTOCORRELATION OF SATCOM ON-THE-MOVE BLOCK-AGE CHANNELS

As reported in [18] and derived in section 4.2, the correlation coefficient of the output of the two-state Markov process is exponential, taking the form

$$R[n] = R[1]^n. \quad (29)$$

The complete correlation coefficient function is known, then, if one can determine $R[1]$, the correlation coefficient at one sample offset.

Let X be a random variable denoting the states of the two-state Markov process. Using +1, -1 as the outputs of the good and bad states, respectively, the correlation coefficient at one sample offset can be written in terms of the mean and variance of the state output:

$$R[1] = \frac{2p_{bb}(1 - \overline{X}) - 4\pi_b + \sigma^2}{\sigma^2}. \quad (30)$$

where p_{bb} is a transition probability in Figure 16 and \overline{X} and σ^2 are the mean value and variance, respectively, of the channel state. The value π_b represents the steady-state probability of being in the blocked state.

An expression equivalent to (30) can be written using reference only to the “good” state \mathbf{g} . We choose to write the expression in terms of \mathbf{b} since the observed blockage distributions tend to agree better with the two-state model than do the connection distributions.

All variables on the right-hand side of (30) are parameters that may be directly estimated from the measured sequence of state outputs. Using estimates of these parameters, we evaluate the suitability of the

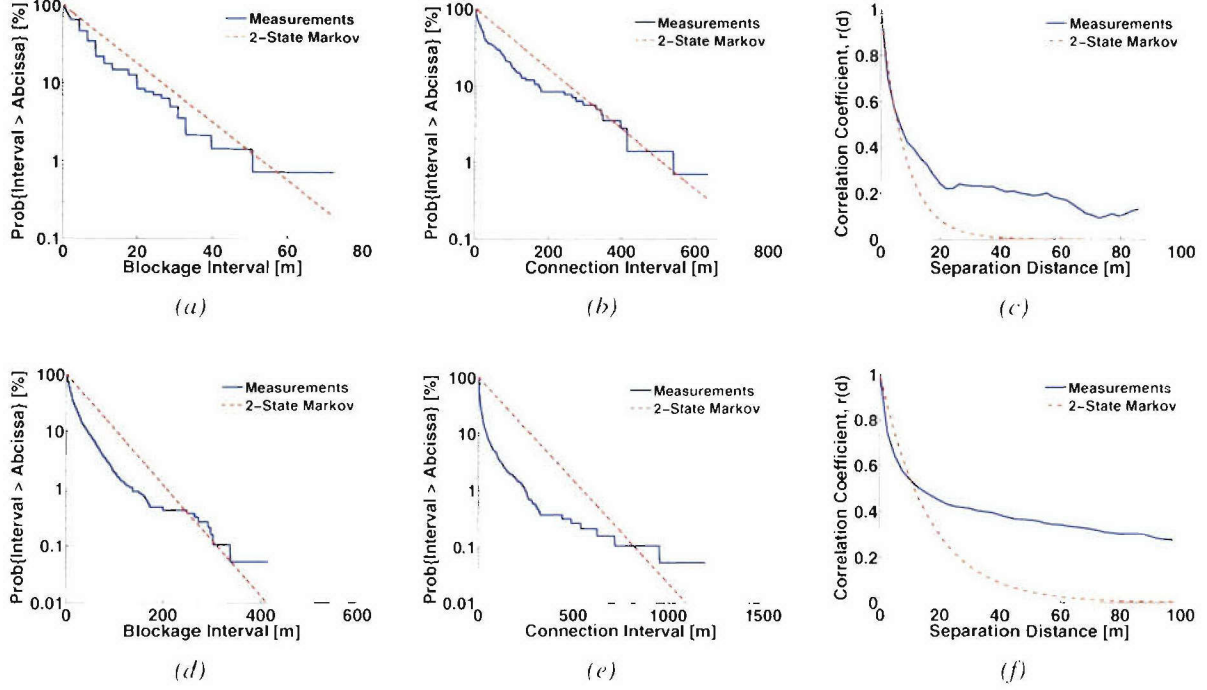


Figure 23. Summary of two-state Markov model with correlation coefficients. Plots (a)–(c) in the top row are representative of data sets for which the two-state model is appropriate. Plot (d)–(f), however, are typical of cases in which the two-state Markov model does not reflect system behavior since the cdf's fall off more rapidly than the exponential expressions given in (1) and (2). The exponential curves for the Markov correlation coefficient model in (c) and (f) are generated using (29) and (30) rather than directly fitting the measured correlation coefficient.

model based on how well the correlation coefficient predicted by (30) matches the correlation coefficient of the measurements.

We estimate values for the mean (\bar{X}) and variance (σ^2) directly from measured state outputs represented by

$$x_i = \begin{cases} +1 & s_{\text{dB}} \geq s_{\text{thresh}} \\ -1 & s_{\text{dB}} < s_{\text{thresh}} \end{cases} \quad (31)$$

where s_{dB} is the measured signal strength in decibels. The results here use a threshold

$$s_{\text{thresh}} = s_{\text{LOS}} - 5 \text{ dB}, \quad (32)$$

where s_{LOS} is the signal strength of the line-of-sight, *i.e.*, unblocked, path to the satellite. The mean is therefore computed as

$$\bar{x} = \frac{1}{N} \sum_{i=0}^{N-1} x_i. \quad (33)$$

The variance is computed from the sampled state outputs using the unbiased estimate

$$\sigma_x^2 = \frac{1}{N-1} \sum_{i=0}^{N-1} (x_i - \bar{x})^2. \quad (34)$$

The value for π_b is estimated from the blockage fraction, *i.e.*, the fraction of the output state samples for which $x_i = -1$. The value for p_{bb} is estimated from the blockage cdf by performing a least-squares linear fit of (1) to the logarithm of the measured cdf of blockage durations.

The plots in Figure 23 show the results of this analysis. The dashed red lines are fit to the cdf of blockage durations in Figure 23(a) and (d) using (1). Similarly, the cdf of connection durations in Figure 23(b) and (e) are compared to the ideal distribution given by (2). The solid blue curves in Figure 23(c) and (f) represent the computed correlation coefficient given by

$$r[k] = \frac{\frac{1}{N-1} \sum_{i=0}^{N-1} (x_i - \bar{x}) (x_{i+k} - \bar{x})}{\sigma_x^2}. \quad (35)$$

For purposes of this analysis, we consider the correlation coefficient predicted by (29), (30) to be a good match if the predicted curve, indicated by the red dashed line in Figure 23(c) and (f), matches the measured correlation coefficient curve for $0.5 \leq r[k] \leq 1$.

The plots in the top row of Figure 23 are typical of cases in which the data is consistent with the two-state Markov model according to our criteria, while the bottom row is representative of cases for which the two-state model is not appropriate. Twelve of the 45 data sets analyzed are similar to Figure 23(a)–(c), meaning that the two-state Markov process is valid under certain circumstances. Since the two-state model is not universally applicable, however, more complex models, such as the Gilbert-Elliott model or a three-state Markov model, may be appropriate.

The separation distance at which the channel decorrelates with itself is a useful measure when considering the use of cooperating mobile terminals. Schodorf and Wu [18] use the two-state model to evaluate diversity reception among mobile satellite terminals.

If one considers the channel to be decorrelated when $r[k] \leq 0.5$, we can summarize the ranges of decorrelation distances for this campaign as shown in Figure 24. Shorter decorrelation distances mean that mobile ground terminals can be spaced more closely together and still benefit from the advantages of some form of diversity for reception or transmission. For example, cooperating ground terminals can be grouped more closely in Cambridge, classified as light urban, than they can be in Boston, which falls in the dense urban grouping.

4.4 SUMMARY

In this chapter we evaluate the properties of the SATCOM on-the-move channel when multiple terminals are used in a cooperative manner. Since neighboring terminals are able to offer the use of additional SATCOM resources, the effective connectivity to a cluster of ground nodes is improved.

We find that the two-state Markov model provides a reasonable blockage model for nodes that are in a cooperating cluster of ground terminals. The measurements agree quite well with the model for blockage

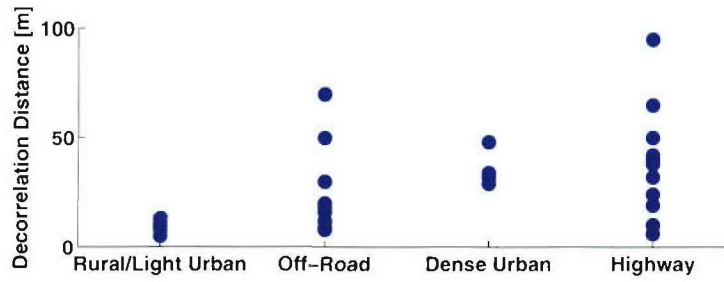


Figure 24. Measured decorrelation distances. The rural/light urban areas include measurements made in Cambridge, Boston's Back Bay, and rural, tree-lined roads through Concord, MA, and other Boston suburbs. The off-road grouping includes the measurements made at Ft. Devens. The dense urban grouping includes Boston, MA, and Hartford, CT, and the highway grouping includes multi-lane freeways.

probabilities and mean blocked and open durations for multiple terminals that are scattered with independent channel blockages. When channel blockages are not independent, such as in a vehicle convoy, the advantage of having multiple terminals degrades somewhat.

We derive the correlation coefficient of an N -state Markov model. The exponential characteristic of the correlation coefficient for the two-state model is the same regardless of what two unique values are chosen as state outputs. The model agrees reasonably well in about 25% of the data sets. The best fits occur when the distribution functions also agree well with the two-state model. It is possible that an improved correlation model would agree with a larger volume of the data sets.

5. CONCLUSION

5.1 REPORT SUMMARY

The new data sets presented in this report include measurements from a terminal that can recover from long outage periods. Due to the enhanced terminal capability, the data sets include regions that were not previously measurable due to limitations of the measurement terminal. Expanded data collection areas provide additional statistics of blockage behavior for urban and highway data. Homogeneity of terrain suggests a partitioning of the data sets based on terrain features. We see that the blockage statistics in the Boston financial district differ from the composite view of the entire city. We analyze the statistics of the new measurement data and find that the two-state Markov model is not ideal, but it provides a reasonable fit to the data over a wide range of operating conditions.

Satellite communication to a cluster of ground vehicles containing multiple SATCOM nodes can be improved by using all SATCOM links in a cooperative manner. The cluster is effectively blocked only when all available satellite links are simultaneously blocked. We analyze the theoretical performance gains that can be achieved by these clusters of cooperating nodes. Using the measurement data, we find that the theory predicts the improved performance quite well if the SATCOM channel outages experienced by each node are independent.

Convoy configurations, however, do not achieve the full performance benefits of cooperating ground nodes since the channel realizations experienced by each node are not fully independent. To characterize this channel correlation, we derived the correlation coefficient for the two-state Markov model and find that its exponential characteristic matches approximately 25% of the data sets evaluated. We also compute the empirical decorrelation distance from the raw data. The decorrelation distance can be used as a guideline for how far apart vehicles in convoy must be separated to achieve significant performance gains by using multiple terminals.

5.2 FUTURE WORK

The SATCOM on-the-move channel experiences outages due to buildings, trees, terrain, and other objects that obstruct the terminal's path to the satellite. Alternate network paths from the satellite to a specific ground terminal may be used to mitigate the adverse effects of link outage. We consider the case in which there are multiple terminals operating in a locality such that a ground network among a group of mobile terminals is fully connected. Satellite transmissions are available to all ground terminals and that terrestrial radio transmissions are available to all nearby ground terminals. Networks that use broadcast media at the physical layer are not easily represented using traditional graph theory, and the analysis must therefore be adjusted.

A number of detailed approaches may be used to improve the overall performance of a network by using all links cooperatively. Static routing, dynamic routing, and network coding are of interest in this context. Static routing refers to the case in which packets are routed through the terrestrial network based

on pre-determined rules. Dynamic routing schemes adjust the routing rules based on observed outage conditions so that data is sent terrestrially to nodes that experienced SATCOM outages. Recent progress in network coding suggests that algebraic functions over a finite field can be used to form linear combinations of packets before sending them out over the wire. Packets may be combined and sent over the links in such a way that the data may be recovered if the fraction of packets received meets some minimum criteria.

There are limitations to these data sets collected during this measurement campaign. The models that were derived from these data might be limited as well. All of the measurements are taken from the same satellite at locations that were within about 0.6 degree of latitude and 1.6 degrees of longitude. As a result, the measurements and models may be biased to these operating conditions. Measurements using satellites at different locations in the sky are needed to generalize the results.

There are fewer satellites available than points of interest in the sky for development of a generalized blockage model. One could use a three-dimensional model of the buildings and trees to estimate outage locations. Because multipath reception is essentially eliminated by the highly directional SATCOM antenna, optical methods such as ray tracing would be used to determine outage locations for ground nodes. These shadowed locations would be compared to measurements made during the previous measurement campaign. The channel blockage statistics obtained through measurement and simulation could also be compared.

Using the verified simulation model, outage profiles could be determined for arbitrary satellite locations. Simulations would be used to generalize the blockage channel model for different elevation angles.

REFERENCES

1. J. B. Schodorf, "EHF satellite communications on the move: Experimental results," Technical Report TR-1087, MIT Lincoln Laboratory, August 2003.
2. E. A. Faulkner, A. P. Worthen, J. B. Schodorf, and J. D. Choi, "Interactions between TCP and link layer protocols on mobile satellite links," in *IEEE Military Communications Conference*, vol. 1, 2004.
3. E. A. Faulkner, "Interactions between TCP and link layer protocols on mobile satellite links," Master's thesis, Massachusetts Institute of Technology, Cambridge, MA, May 1993.
4. J. T. Delisle. Private communications.
5. C. Loo and J. S. Butterworth, "Land mobile satellite channel measurements and modeling," *Proceedings of the IEEE*, vol. 86, no. 7, pp. 1442 – 1463, 1998.
6. A. Abdi, W. C. Lau, M.-S. Alouini, and M. Kaveh, "A new simple model for land mobile satellite channels: first- and second-order statistics," *IEEE Transactions on Wireless Communications*, vol. 2, no. 3, 2003.
7. F. Dovis, R. Fantini, M. Mondin, and P. Savi, "Small-scale fading for high-altitude platform (HAP) propagation channels," *IEEE Journal on Selected Areas in Communications*, vol. 20, no. 3, pp. 641 – 647, 2002.
8. M. Döttling, A. Jahn, D. Didascalou, and W. Wiesbeck, "Two- and three-dimensional ray tracing applied to the land mobile satellite (LMS) propagation channel," *IEEE Antennas and Propagation Magazine*, vol. 43, no. 6, pp. 27 – 37, 2001.
9. C. Oestges and D. Vanhoenacker-Janvier, "Propagation modeling and system strategies in mobile-satellite urban scenarios," *IEEE Transactions on Vehicular Technology*, vol. 50, no. 2, pp. 422 – 429, 2001.
10. E. N. Gilbert, "Capacity of a burst-noise channel," *Bell System Technical Journal*, pp. 1253 – 1265, September 1960.
11. L. E. Braten and T. Tjelta, "Semi-Markov multistate modeling of the land mobile propagation channel for geostationary satellites," *IEEE Transactions on Antennas and Propagation*, vol. 50, no. 12, 2002.
12. F. P. Fontan, M. Vazquez-Castro, C. E. Cabado, J. P. Garcia, and E. Kubista, "Statistical modeling of the LMS channel," *IEEE Transactions on Vehicular Technology*, vol. 50, no. 6, pp. 1549 – 1567, 2001.
13. H. Yao, "EHF satellite communications-on-the-move: Blockage channel modeling," Technical Report TR-1098, MIT Lincoln Laboratory, November 2004.
14. Massachusetts Geographic Information System. <http://www.mass.gov/mgis>.
15. E. Lutz, D. Cygan, M. Dippold, F. Dolainsky, and W. Papke, "The land mobile satellite communication channel-recording, statistics, and channel model," *IEEE Transactions on Vehicular Technology*, vol. 40, no. 2, pp. 375 – 386, 1991.
16. W. C. Jakes, ed., *Microwave Mobile Communications*. IEEE Press, 1994.

17. H. Yao. Private communications.
18. J. B. Schodorf and P. H. Wu, "Diversity reception for blockage mitigation in EHF land mobile satellite communications systems," in *Proceedings of the 54th Vehicular Technology Conference*, vol. 1, 2001.
19. A. Leon-Garcia, *Probability and Random Processes for Electrical Engineering*. Reading, Mass.: Addison-Wesley, 1989.

REPORT DOCUMENTATION PAGE				Form Approved OMB No. 0704-0188	
Public reporting burden for this collection of information is estimated to average 1 hour per response, including the time for reviewing instructions, searching existing data sources, gathering and maintaining the data needed, and completing and reviewing this collection of information. Send comments regarding this burden estimate or any other aspect of this collection of information, including suggestions for reducing this burden to Department of Defense, Washington Headquarters Services, Directorate for Information Operations and Reports (0704-0188), 1215 Jefferson Davis Highway, Suite 1204, Arlington, VA 22202-4302. Respondents should be aware that notwithstanding any other provision of law, no person shall be subject to any penalty for failing to comply with a collection of information if it does not display a currently valid OMB control number. PLEASE DO NOT RETURN YOUR FORM TO THE ABOVE ADDRESS.					
1. REPORT DATE (DD-MM-YYYY) 07-12-2006		2. REPORT TYPE Technical Report		3. DATES COVERED (From - To)	
4. TITLE AND SUBTITLE Channel Characterization for EHF Satellite Communications on the Move				5a. CONTRACT NUMBER FA8721-05-C-0002	
				5b. GRANT NUMBER	
				5c. PROGRAM ELEMENT NUMBER	
6. AUTHOR(S) W.M. Smith				5d. PROJECT NUMBER	
				5e. TASK NUMBER	
				5f. WORK UNIT NUMBER	
7. PERFORMING ORGANIZATION NAME(S) AND ADDRESS(ES) MIT Lincoln Laboratory 244 Wood Street Lexington, MA 02420-9108				8. PERFORMING ORGANIZATION REPORT NUMBER TR-1109	
9. SPONSORING / MONITORING AGENCY NAME(S) AND ADDRESS(ES) Barry S. Perlman, Ph.D. US Army Research, Development and Engineering Command Communications-Electronics Research, Development and Engineering Course Ft. Monmouth, NJ 07703-5201				10. SPONSOR/MONITOR'S ACRONYM(S) SFAE-C3T-WINT-TMD	
				11. SPONSOR/MONITOR'S REPORT NUMBER(S) ESC-TR-2006-062	
12. DISTRIBUTION / AVAILABILITY STATEMENT Approved for public release; distribution is unlimited.					
13. SUPPLEMENTARY NOTES					
14. ABSTRACT In addition to long signal propagation delays, the mobile satellite terminal in a land-mobile satellite communications system is subject to channel impairments imposed by the terrestrial environment. Statistical channel models are needed for protocol development and performance evaluation of systems for satellite communications (SATCOM) on the move. Experimental measurements were made in and around Boston, MA, using a prototype system for SATCOM on the move. The measurements characterize the 20 GHz down-link signal and were made in the fall and winter months of 2004. The elevation angle to the satellite was approximately 36°. This report covers the measurement campaign, initial single-terminal channel modeling, and multi-terminal channel models relevant for cooperating ground terminals. The data sets are analyzed for the statistical properties of the channel state. The channel is considered to be "open" when a clear path exists to the satellite and "blocked" when there is an obstruction in the path that prevents the successful transfer of information from transmitter to receiver. For the single-channel analysis, three operational environments were previously classified as urban, rural, or open. We propose two new operational categories: open highway and dense urban. The addition of these categories is based on a natural partitioning of the experimental data. The open highway channel model contains very long open intervals, 310 m on average, and is blocked 5% of the time. The dense urban environment, on the other hand, consists of tall, closely spaced buildings. In this environment, the average blockage duration is 130 m and the channel is blocked 89% of the time. We evaluate the suitability of Markov state models to accurately reflect the channel behavior. The effectiveness of using multiple terminals to maximize the use of a single satellite depends on the correlation properties of the blockage events experienced by each mobile ground terminal. Terminal groups with uncorrelated channel outages are able to maximize the use of the satellite since there is a lower probability that all terminals are simultaneously blocked. The autocorrelation properties of the blockage channel state determine how closely spaced the ground terminals may be in order to reap the full benefits of spatial diversity. We derive the correlation coefficient of a multiple-state Markov channel with arbitrary state outputs. The correlation coefficient of the two-state model is found to be exponential, regardless of the state output values. We find the empirical channel decorrelation distance to be from 10 m to 100 m, depending on the operating environment. The empirical blockage probability reduces from 40% to 5% for a cluster of four randomly moving ground terminals in a light urban environment.					
15. SUBJECT TERMS					
16. SECURITY CLASSIFICATION OF:			17. LIMITATION OF ABSTRACT	18. NUMBER OF PAGES	19a. NAME OF RESPONSIBLE PERSON
a. REPORT Unclassified	b. ABSTRACT Unclassified	c. THIS PAGE Unclassified	None	58	19b. TELEPHONE NUMBER (include area code)